

Title: BDNF-TrkB signaling in oxytocin neurons contributes to maternal behavior

Running title: BDNF-TrkB signaling in oxytocin neurons

Kristen R. Maynard, PhD¹, John W. Hobbs, BA¹, Badoi N. Phan, BS¹, Amolika Gupta¹, Sumita Rajpurohit¹, Courtney Williams, BA¹, Nina Rajpurohit, BA¹, Joo Heon Shin, PhD¹, Andrew E. Jaffe, PhD^{1,2,3,4}, Keri Martinowich, PhD^{1,5}

¹Lieber Institute for Brain Development, Johns Hopkins Medical Campus, Baltimore, Maryland, 21205

²Department of Biostatistics, Johns Hopkins Bloomberg School of Public Health, Baltimore, MD, USA.

³Center for Computational Biology, Johns Hopkins University, Baltimore, MD, USA.

⁴Department of Mental Health, Johns Hopkins University, Baltimore, MD, USA.

⁵Departments of Psychiatry & Behavioral Sciences, and Neuroscience, Johns Hopkins University School of Medicine, Baltimore, MD, USA.

Correspondence:

Keri Martinowich

Lieber Institute for Brain Development

855 North Wolfe Street, Suite 300

Baltimore, MD, 21205.

keri.martinowich@libd.org

(410) 955-1510

Abstract:

Brain-derived neurotrophic factor (*Bdnf*) transcription is controlled by several promoters, which drive expression of multiple transcripts encoding an identical protein. We previously reported that BDNF derived from promoters I and II is highly expressed in hypothalamus and is critical for regulating aggression in male mice. Here we report that BDNF loss from these promoters causes reduced sexual receptivity and impaired maternal care in female mice, which is concomitant with decreased oxytocin (*Oxt*) expression during development. We identify a novel link between BDNF signaling, oxytocin, and maternal behavior by demonstrating that ablation of TrkB selectively in OXT neurons partially recapitulates maternal care impairments observed in BDNF-deficient females. Using translating ribosome affinity purification and RNA-sequencing we define a molecular profile for OXT neurons and delineate how BDNF signaling impacts gene pathways critical for structural and functional plasticity. Our findings highlight BDNF as a modulator of sexually-dimorphic hypothalamic circuits that govern female-typical behaviors.

Introduction:

Brain-derived neurotrophic factor (BDNF) is an activity-dependent neurotrophin that binds the receptor tropomyosin receptor kinase B (TrkB) to mediate many aspects of brain plasticity (Andero, Choi, & Ressler, 2014; Chao, Rajagopal, & Lee, 2006; Lu, 2003). Early social experience, especially maternal care, strongly modulates BDNF levels in rodents and *BDNF* methylation in humans (Branchi et al., 2013; Liu, Diorio, Day, Francis, & Meaney, 2000; Suzuki et al., 2011; Unternaehrer et al., 2015). A unique aspect of BDNF regulation is transcription by nine distinct promoters that generate ~22 transcripts encoding an identical BDNF protein (**Fig. 1a**) (Aid, Kazantseva, Piirsoo, Palm, & Timmusk, 2007; Pruunsild, Kazantseva, Aid, Palm, & Timmusk, 2007; Timmusk et al., 1993; West, Pruunsild, & Timmusk, 2014). Alternative *Bdnf* promoters allow for tight temporal, spatial, and stimulus-specific BDNF expression, which is critical for modulating plasticity in specific neural circuits (Baj et al., 2012; Baj, Leone, Chao, & Tongiorgi, 2011; Pattabiraman et al., 2005; Timmusk, Belluardo, Persson, & Metsis, 1994). We have shown that *Bdnf* promoters I and II significantly contribute to BDNF expression in the hypothalamus and that selective disruption of BDNF expression from these promoters, but not others, causes enhanced aggression and elevated mounting in males (Maynard et al., 2016). While it is established that BDNF modulates social behavior in males (Chan, Unger, Byrnes, & Rios, 2006; Ito, Chehab, Thakur, Li, & Morozov, 2011; Lyons et al., 1999), no studies to-date have investigated the role of BDNF-TrkB signaling in influencing female-typical social behaviors, particularly mating and maternal care. This is especially surprising given the wealth of literature supporting the converse relationship that reduced maternal care impairs BDNF signaling in offspring (Branchi et al., 2013; Liu et al., 2000; Unternaehrer et al., 2015).

BDNF and its receptor TrkB are highly expressed in the paraventricular nucleus (PVN) of the hypothalamus and influence the survival and modulation of magnocellular and parvocellular neurons releasing oxytocin (OXT) (Kusano, House, & Gainer, 1999; Moreno, Piermaria, Gaillard, & Spinedi, 2011), a neuropeptide crucial for social behaviors such as pair bonding,

mating, and parenting (Dolen, 2015; Marlin, Mitre, D'Amour J, Chao, & Froemke, 2015; Neumann, 2008). Oxytocin neurons show significant changes in morphology, electrophysiology, and synaptic plasticity during female-typical social behaviors such as parturition and lactation (Stern & Armstrong, 1998; Theodosis, 2002), but the mechanisms mediating this activity-induced structural and functional plasticity—and whether they extend to other maternal behaviors—are not completely understood. Furthermore, while genes co-expressed with *Oxt* transcripts have been identified (Romanov et al., 2017; Yamashita, Glasgow, Zhang, Kusano, & Gainer, 2002), a complete molecular signature of OXT neurons in sexually mature females has not yet been defined. Given that BDNF is a robust modulator of gene expression and has been associated with remodeling of GABA_A receptors in hypothalamic neuroendocrine cells (Choe et al., 2015; Hewitt & Bains, 2006), we investigated the role of BDNF in regulating gene transcription and plasticity in OXT neurons during female-typical social behaviors. Here we delineate how disruption of BDNF-TrkB signaling in female mice impacts maternal care and OXT neuron gene expression. We define the molecular identity of OXT neurons and demonstrate novel roles for BDNF signaling in the modulation of female-typical social behaviors and OXT neuron plasticity.

Methods:

Animals

Mice with disruption of BDNF production from promoters I, II, IV, or VI (*Bdnf*-e1, -e2, -e4, -e6 mice *-/-*, respectively) were generated as previously described (Maynard et al., 2016) and backcrossed to C57BL/6J at least 12x. Briefly, an enhanced green fluorescent protein (eGFP)-STOP cassette was inserted upstream of the respective 5'UTR splice donor site of the targeted exon. For example, in *Bdnf*-e1, -e2, -e4, and -e6 *-/-* mice, transcription is initiated from promoter I, II, IV, or VI, producing a 5'UTR-eGFP-STOP-*Bdnf* IX transcript, which leads to GFP production in lieu of BDNF from the targeted promoter (**Fig. 1b**). Sexually mature female WT and *Bdnf* *-/-* mice were used for all behavioral experiments. We selectively ablated TrkB in OXT-

expressing cells by crossing mice driving Cre-recombinase under control of the endogenous *Oxt* promoter, (*Oxt*^{tm1.1(cre)Dolsn}; referenced in text as *Oxt*^{Cre}, stock #024234, Jackson Labs, Bar Harbor, ME (Wu et al., 2012)), to mice carrying a *loxP*-flanked *TrkB* allele⁹ (strain fB/fB, referenced in text as *TrkB*^{flox/flox} (Grishanin et al., 2008)). *Oxt*^{Cre}/*TrkB*^{flox/flox} served as the experimental group while *TrkB*^{flox/flox} mice were used as controls (**Fig. 3b**). For RiboTag experiments in wild-type OXT neurons, *Oxt*^{Cre} mice were crossed to the RiboTag mouse (B6N.129-Rpl22^{tm1.1Psam/J}; referenced in text as Rpl22^{HA}, stock #011029, Jackson Labs (Sanz et al., 2009)), which expresses a hemagglutinin (HA) tag on the ribosomal protein RPL22 (RPL22^{HA}) under control of Cre-recombinase (**Fig. 4a**). For RiboTag experiments in interneurons, Rpl22^{HA} mice were also crossed to mice expressing Cre-recombinase under control of the endogenous cortistatin promoter (*Cort*^{tm1(cre)Zjh/J}; referenced in text as CST^{Cre}, stock# 010910, Jackson Labs (Taniguchi et al., 2011)). For RiboTag experiments in *Bdnf-e1* -/- and controls (**Fig. 5a**), AAV1-DIO-RPL22^{HA}-GFP (generous gift of McKnight lab (Sanz et al., 2015); packaged by Penn Vector Core, University of Pennsylvania, Philadelphia, PA), was virally injected into *Bdnf-e1*; *Oxt*^{Cre} mice that were triple crossed to a mouse expressing tdTomato under control of Cre-recombinase (B6.Cg-Gt(ROSA)26Sor^{tm14(CAG-tdTomato)Hze/J}, referred to as tdTom, stock # 007914, Jackson Labs).

Adult female mice were housed in a temperature-controlled environment with a 12:12 light/dark cycle and *ad libitum* access to food and water. Prior to experimentation, mice were grouped housed based on genotype. For experiments in postpartum mothers, mice were impregnated by CD1 males (21-24g; Envigo, Frederick, MD) and then isolated into their own cages 3-4 days prior to parturition. For experiments in virgin females, experimental animals were isolated into individual cages 24 hours prior to pup retrieval testing. Adult CD1 females were used for generating foreign pups (P0 to P1). All experimental animal procedures were approved by the Sobran Biosciences Institutional Animal Care and Use Committee.

Immunohistochemistry

For verification of RPL22^{HA} expression in *Bdnf-e1*; *Oxt^{Cre}*; *tdTom* mice, a representative animal was anesthetized with isoflurane ~3 weeks following intracranial infusion of AAV-DIO-RPL22^{HA}-GFP and transcardially perfused with 4% paraformaldehyde (PFA) in phosphate buffer saline (PBS) pH 7.4. The brain was removed, post-fixed overnight in PFA at 4°C, cryoprotected in 30% sucrose, and cut at 50µm on a microtome (Leica, Wetzlar, Germany) equipped with a freezing stage (Physitemp, Clifton, NJ). Free-floating slices were permeabilized with 0.3% Triton/PBS and blocked in 3% Normal Goat Serum (NGS)/0.3% Triton/PBS for 1 hour. Sections were incubated in anti-mouse HA (1:000, MMS-101R, Covance, Princeton, NJ) overnight at 4°C. The following day, sections were rinsed 3 x 10 minutes in PBS and incubated in goat anti-mouse Alexa 647 (Cat # A-21235, Thermo-Fisher Scientific, 1:750) for 1 hour at room temperature. Slices were washed 3 x 10 minutes with PBS, incubated in DAPI at 1:5000, and mounted using Fluoromount G (Cat # 0100-01 Southern Biotechnology, Birmingham, Alabama).

For OXT and cFOS quantification, adult WT and *Bdnf-e1* ^{-/-} postpartum mice were sacrificed 2 hours following pup retrieval testing (1 day after parturition) and transcardially perfused with 4% PFA. Brains were removed, post-fixed overnight in PFA at 4°C, cryoprotected in 30% sucrose, and cut at 50µm on a microtome equipped with a freezing stage. For fluorescence co-labeling experiments, free-floating sections were permeabilized with 0.5% Tween/PBS (PBST) for 30 minutes and blocked with 2.5% Normal Donkey Serum (NDS)/2.5% NGS/0.5% Tween in PBS for ~5 hours. Sections were then incubated with anti-mouse OXT (1:100; generous gift of Dr. Harold Gainer; NIH, Bethesda (Ben-Barak, Russell, Whitnall, Ozato, & Gainer, 1985)) and anti-rabbit cFOS (1:1000, Cat # ABE457 Millipore, Massachusetts, USA) in block overnight at 4°C. Sections were rinsed 3 x 20 minutes with PBST, incubated in donkey anti-rabbit Alexa 488 (Cat # A-21206 ThermoFisher Scientific, 1:1000) and goat anti-mouse Alexa 647 (1:750) for 2 hours at room temperature, and then rinsed again for 4 x 15 minutes. Before coverslipping with Fluoromount G sections were incubated with DAPI at 1:5000 for 20 minutes to label nuclei.

Image Acquisition and Analysis

WT and Bdnf-e1 ^{-/-} paraventricular nuclei (PVN, n=6-9 images per animal, n=3 animals per genotype, n=48 total) were tile imaged in z-series at 20x magnification using a Zeiss LSM 700 microscope (Carl Zeiss, Oberkochen, Germany). Images were stitched in x,y using Zen software (Zeiss) and analyzed using custom MATLAB and R scripts. PVN regions were segmented to include the bulk of OXT-expressing neurons excluding the third ventricle and ventricular zone cells. Adaptive 3D segmentation was performed on image stacks using the CellSegm MATLAB toolbox (Hodneland, Kogel, Frei, Gerdes, & Lundervold, 2013) of the PVN region (filter radius = 11px, adaptive threshold = 1e-5). Individual nuclei were further split and separated using the DAPI channel and the 3D watershed function in MATLAB as previously described (Ram, Rodriguez, & Bosco, 2012) to characterize OXT and cFOS co-localization. Statistical analyses of extracted co-localization and shape characteristics were performed in R using mixture models to account for repeated measurements of the PVN region from the same animal. All processing and analysis scripts are available on GitHub (https://github.com/LieberInstitute/cFOS_OXT_Image_Analysis) and data are available upon request from the authors.

RNA extraction and qPCR

WT and Bdnf-e1 ^{-/-} postpartum mice were cervically dislocated and hypothalami were collected on ice. RNA was extracted using TRIzol (Life Technologies, Carlsbad, CA), purified using RNeasy minicolumns (Qiagen, Valencia, CA), and quantified using a Nanodrop spectrophotometer (Agilent Technologies, Savages, MD). RNA was then normalized in concentration and reversed transcribed using Superscript III (Life Technologies). Quantitative PCR (qPCR) for oxytocin (*Oxt*) and the oxytocin receptor (*OxtR*) was performed using a Realplex thermocycler (Eppendorf, Hamburg, Germany) with GEMM mastermix (Life Technologies) and 40ng of synthesized cDNA. Individual mRNA levels were normalized for

each well to *Gapdh* mRNA levels. Taqman probes were commercially available from Life Technologies (Mm01329577_g1, Mm01182684_m1, 4352932E).

RNAscope *in situ* hybridization

An adult WT virgin female was cervically dislocated and the brain was removed from the skull, flash frozen in isopentane, and stored at -80°C. Brain tissue was equilibrated to -20°C in a cryostat (Leica, Wetzlar, Germany) and serial sections of paraventricular nucleus (PVN) were collected at 16µm. Sections were stored at -80°C until completion of the RNAscope assay. We performed *in situ* hybridization with RNAscope technology utilizing the RNAscope Fluorescent Multiplex Kit (Cat # 320850 Advanced Cell Diagnostics, Hayward, California) according to manufacturer's instructions. Briefly, tissue sections were fixed with a 10% neural buffered formalin solution (Cat # HT501128 Sigma-Aldrich, St. Louis, Missouri) and pretreated with protease IV for 20 minutes. Sections were incubated with a custom-designed Channel 1 *Oxt* probe (Cat # 493171 Advanced Cell Diagnostics, Hayward, California) and a commercially available *Ntrk2* (TrkB) probe (Cat # 423611-C2 Advanced Cell Diagnostics, Hayward, California). Probes were fluorescently labeled with ORANGE (Excitation 550 nm; Emission 580 +/- 10 nm) or GREEN (Excitation 488 nm; Emission 540 +/- 10 nm) fluorophores using the Amp 4 Alt B-FL. Confocal images were acquired in z-series at 40x magnification using a Zeiss 700LSM confocal microscope. For co-localization of *Gabra2* and *Cckar* transcripts with *Oxt* transcripts, brains were harvested from representative adult virgin *Bdnf-e1* +/+; *Oxt*^{Cre}; tdTom and *Bdnf-e1* -/-; *Oxt*^{Cre}; tdTom mice and subjected to the protocol described above. Sections were incubated with commercially available probes for *Gabra2* and *Cckar* (Cat # 435011 and 313751, ACD).

Postpartum Pup Retrieval

Adult female mice (7-8 weeks old) were impregnated by CD1 males and single-housed with a compact cotton nestlet 4-5 days before parturition. Upon parturition, date of birth, pup number, and nest quality was recorded without disturbing cages. Pup survival was monitored until P3.

Postpartum pup retrieval was performed at P1 as previously described (Carlier, Roubertoux, & Cohen-Salmon, 1982). Briefly, dams were isolated from the homecage for ~1 min while pups were carefully moved 20 cm from the nest. Dams were returned to the homecage and behavior was recorded for 15 minutes using the CaptureStar software (Clever Systems, Reston, VA). Maternal behavior was scored using both quantitative and qualitative scales with experimenter blinded to genotype. Quantitative measurements were adapted from Carlier et al. 1982 and included latency to first contact, latency to first retrieval, duration of carrying first pup, duration of nesting with first pup, number of move-aways from pups without retrieving, and duration of nesting with pups after completing retrieval (Carlier et al., 1982).

Qualitative measurements included indices for maternal behavior, abnormal behavior, pup retrieval, and global parental type. For maternal behavior index (0 to 5), dams received one point for each observed affiliative behavior, including pup contact, pup carrying, completed pup retrieval (i.e. bringing all pups back to nest), nurturing (licking, crouching, or nesting with pups for at least 1 minute), and covering pups with nesting. For abnormal behavior index (0 to 5), dams received one point for each observed harmful or disorganized behavior, including kicking pups, biting pups, failing to retrieve all pups, repeatedly carrying pups (i.e. retrieving a pup to the nest, but then moving it out again), and misplaced retrieving (i.e. bringing pups to a random location). For retrieval index (1 to 4), dams were ranked as following: 1-no retrieval (ignore pups), 2-partial pup retrieval (retrieve some, but not all pups), 3-complete pup retrieval (retrieve all pups, but may subsequently scatter or fail to nest with pups), 4-retrieval all pups and nurture (nest for at least 2 minutes with pups). For global maternal type, dams were ranked as the following: 1-parenting (retrieve all pups to nest or delivered nest to pups; nurtured or nested for at least 1 minute), 2-disorganized parenting (retrieve all pups to nest, but scatter, kick, or repeatedly pick-up), 3-partial parenting (incomplete retrieval, but no scattering or repeated pick ups), 4-disorganized partial parenting (incomplete retrieval with scattering, kicking, or repeated pick ups), 5-non-parenting (no retrieval; ignore pups), 6-attack (aggressive biting).

Virgin Pup Retrieval

Virgin female mice were single-housed with a compact nestlet ~24 hours before testing. During testing, three foreign pups (P0-P1) obtained from time-pregnant CD1 females (Envigo) were placed in the homecage opposite to the majority of nesting material. Behavior was recorded for 15 minutes using CaptureStar software, unless a pup was attacked, in which case the experiment was terminated immediately. Videos were scored blinded to genotype using the same scales described above for postpartum pup retrieval, including maternal behavior, abnormal behavior, and retrieval indices. For virgins, global parental type was modified to the following criteria based on differences in styles observed between postpartum and virgin females: 1-parenting (retrieve all pups to nest or delivered nest to pups; nurtured or nested for at least 1 minute), 2-partial parenting (retrieve some but not all pups to nest), 3-irregular parenting (no retrieval but nurturing such as crouching and licking), 4-non-parenting (no retrieval; ignore pups), 5-attack (aggressive biting).

Behavioral Statistics

Statistical analysis was conducted using GraphPad Prism Software (La Jolla, CA) or R for Cox regression, Mann-Whitney-Wilcoxon rank sum test, multinomial regression, or log rank survival tests where appropriate. Comparisons between two groups were performed using unpaired Student's t-test or Mann-Whitney tests where appropriate. Comparisons between three or more groups were performed using ANOVA with Bonferroni posthoc tests or Kruskal-Wallis with Dunn's multiple comparisons. Data are presented as mean \pm SEM and statistical significance was set at *P < 0.05, **P < 0.01, &P < 0.001, and #P < 0.0001.

RiboTag and RNA-sequencing

To identify genes enriched in OXT neurons, hypothalami of Oxt^{Cre}; Rpl22^{HA} mice were collected and flash frozen in isopentane. For each sample (n=3 Input and n=3 IP), five hypothalami were pooled and homogenized according to previously described protocols (Sanz et al., 2013). Thirty microliters of total homogenate were flash frozen and reserved for "Input" samples. Ribosome-

mRNA complexes (“IP” samples) were affinity purified using a mouse monoclonal HA antibody (MMS-101R, Covance, Princeton, NJ) and A/G magnetic beads (88803 Pierce). RNA from Input and IP samples was purified using RNeasy microcolumns (Qiagen, Valencia, CA) and quantified using the Ribogreen RNA assay kit (R11490 Invitrogen). The Ovation RNA Amplification System V2 kit (7102 Nugen, San Carlos, CA) was used to amplify cDNA from 7-8ng of RNA according to manufacturer’s instructions. cDNA was used for qPCR validation for *Oxt* enrichment in IP versus Input samples and to generate sequencing libraries with the Nextera DNA Library Preparation kit. Libraries were sequenced on a HiSeq 3000 according to manufacturer’s instructions. To replicate these results and establish sequencing workflows for lower input samples, we also generated libraries from these exact samples using the Ovation SoLo RNA-seq System Mouse (0502-32 Nugen, San Carlos, CA) according to manufacturer’s instructions from 7-8ng of starting material. Library concentration was quantified using the KAPA Library Quantification Kit (KR0405, KAPA Biosystems, Wilmington, MA). Libraries were sequenced using the MiSeq Reagent Kit v3 (MS-102-3001 Illumina, San Diego, CA) and Nugen Custom SoLo primer.

To compare differentially expressed genes in OXT neurons between control and *Bdnf-e1*^{-/-} females, an adeno-associated viral vector, AAV1-DIO-RPL22^{HA}-GFP was virally injected into the PVN of *Bdnf-e1* ^{+/+}; *Oxt*^{Cre}; tdTom or *Bdnf-e1* ^{-/-}; *Oxt*^{Cre}; tdTom virgin females (**Fig. 5a**). A viral approach was used due to non-Mendelian generation of expected genotypes for *Bdnf-e1*; *Oxt*^{Cre}; Rpl22^{HA} triple crosses. Briefly, mice were anesthetized with isoflurane and mounted on a stereotaxic frame (Kopf, Tujunga, CA). Virus was bilaterally injected into the PVN using a Hamilton syringe at an injection rate of 100nL/min. PVN coordinates were anteroposterior (AP): -0.7mm, mediolateral (ML): ±0.3mm, and dorsoventral (DV): -4.75 mm. Injection volumes were 500nL. Three weeks following surgery, mice were sacrificed and hypothalami were dissected and homogenized individually and processed as described above. IP sequencing libraries (n=3 control and n=3 *Bdnf-e1* ^{-/-}) were prepared using the Ovation SoLo RNA-seq System Mouse

according to manufacturer's instructions from less than 1ng of starting material. Library concentration was quantified using the KAPA Library Quantification Kit (KR0405, KAPA Biosystems, Wilmington, MA). Libraries were sequenced using the MiSeq Reagent Kit v3 (MS-102-3001 Illumina, San Diego, CA) and Nugen Custom SoLo primer.

RNA-seq data processing and analyses

RNA-seq reads from all experiments were aligned and quantified using a common processing pipeline. Reads were aligned to the mm10 genome using the HISAT2 splice-aware aligner (Kim, Langmead, & Salzberg, 2015) and alignments overlapping genes were counted using featureCounts version 1.5.0-p3 (Liao, Smyth, & Shi, 2014) relative to Gencode version M11 (118,925 transcripts across 48,709 genes, March 2016). Read counting mode was used for single end read libraries (SoLo) and fragment counting mode was used for paired end reads (Ovation, Clontech). We analyzed 22,472 genes with reads per kilobase per million counted/assigned (RPKM normalizing to total number of gene counts not mapped reads) > 0.1 in the RiboTag IP versus input analyses and 22,071 genes with RPKM > 0.1 in the control vs. Bdnf-e1 analysis. Differential expression analyses were performed on gene counts using the voom approach (Law, Chen, Shi, & Smyth, 2014) in the limma R/Bioconductor package (Ritchie et al., 2015) using weighted trimmed means normalization (TMM) factors. Differential expression analyses further adjusted for the gene assignment rate / exonic mapping rate, calculated from the output of featureCounts, which reflects the proportion of aligned reads/fragments assigned to genes during counting. Here the total proportion of exonic reads, which typically explains a large proportion of gene count variance (Jaffe et al., 2017) was higher (but not significantly) in IP compared to Input RNA fractions (73.2% versus 66.0%, $t_{df=4}=2.16$, $p = 0.10$). For control vs. Bdnf-e1 experiments, differential expression modeling for genotype effects further adjusted for the \log_2 expression of *Oxt* to adjust for viral transfection differences. Multiple testing correction was performed using the Benjamini-Hochberg approach to control for the false discovery rate (FDR)(Kasen, Ouellette, & Cohen, 1990). Gene set enrichment

analyses were performed using the subset of genes with known Entrez gene IDs using the clusterProfiler R Bioconductor package (Yu, Wang, Han, & He, 2012). All RNA-seq analysis code is available on the GitHub repository https://github.com/LieberInstitute/oxt_trap_seq.

Results:

BDNF derived from promoters I and II regulates maternal care and mating in females

To assess whether *Bdnf*-e1 or -e2 *-/-* postpartum mothers show impairments in parenting behaviors, we first examined pup survival from parturition until postnatal day 3 (P3). There was a significant decrease in the number of surviving pups for *Bdnf*-e1 *-/-* postpartum mothers compared to WT (**Fig. 1c**; $p = 0.00023$; multinomial regression). Survival analysis using Cox regression showed that pups with *Bdnf*-e1 and -e2 *-/-* mothers had a 2.28 and 1.63 times higher probability of death in the first 3 days of life, respectively ($p=1.1e-05$ and $p=0.0028$). To rule out that decreased pup survival in *Bdnf*-e1 *-/-* was due to maternal stress from pup retrieval testing at P1, we examined pup survival in the homecage. In this naturalistic setting, WT and *Bdnf*-e1 *-/-* postpartum mothers were not disturbed following parturition and yet still showed a significant loss of pups compared to WT (**Fig. 1d**; $p=7.53e-06$; log rank test for equal survival). In fact, almost one-third of *Bdnf*-e1 *-/-* postpartum mothers lost their entire litter by P3 (**Fig. 1e**; $F_{2,52} = 4.14$, $p = 0.0215$). Importantly, pup loss was not due to pup genotype as *Bdnf*-e1 *+/-* mothers show normal pup survival and *Bdnf*-e1 and -e2 alleles are not associated with increased lethality (data not shown).

To directly evaluate maternal care in *Bdnf*-e1 and -e2 *-/-* postpartum mothers, we used a classic pup retrieval paradigm (Carlier et al., 1982) and scored maternal style as well as stereotyped parental behaviors. There was a significant decrease in the proportion of *Bdnf*-e1 *-/-* postpartum mothers showing parenting behavior (retrieving and nesting with pups) compared to controls (**Fig. 1f**; Mann-Whitney-Wilcoxon rank sum test, $W=111.5$, Bonferroni corrected $p=0.0466$). This decrease was accounted for by an increase in the proportion of *Bdnf*-e1 *-/-*

postpartum mothers that failed to retrieve or interact with pups (non-parenters). In addition to global parental style, mothers were scored on a number of standard behaviors including nest building (**Fig. 1g**; Kruskal-Wallis statistic = 12.95, $p=0.0015$), latency to first retrieval (**Fig. 1h**; $F_{2,50}= 4.668$, $p =0.0138$), time spent carrying first pup (**Fig. 1i**; $F_{2,46}= 3.414$, $p =0.0415$), and time spent nesting with first pup (**Fig. 1j**; $F_{2,51}= 4.167$, $p =0.0211$). Bonferroni comparisons showed that Bdnf-e1 -/- postpartum mothers were significantly impaired in all these categories compared to WT, while Bdnf-e2 -/- postpartum mothers had milder phenotypes with selective deficiencies in nest building and spending time in the nest with pups. Consistent with a non-parenting style for Bdnf-e1 -/- females, there was a significant decrease in the percentage of postpartum Bdnf-e1 -/- mothers retrieving all pups and nesting for more than 2 continuous minutes (**Fig. 1k**; $F_{2,52}= 3.483$, $p =0.0380$).

Given that postpartum Bdnf-e1 -/- mothers showed striking impairments in maternal care, we also tested Bdnf-e1 -/- virgin females for deficits in pup interaction. We conducted a modified version of the pup retrieval test in which virgin females were single-housed for at least 16 hours and exposed to 3 foreign pups in the homecage. Like Bdnf-e1 -/- postpartum mothers, Bdnf-e1 -/- virgins showed significant impairments in nest building compared to WT (**Fig. 1l**; Mann Whitney, $U= 33$, $p=0.0220$). Bdnf-e1 -/- virgins also showed a reduced maternal index (**Fig. 1m**; Mann Whitney, $U= 28.5$, $p=0.0092$) and a strong trend for an elevated abnormal parenting index (**Fig. 1n**; Mann Whitney, $U = 39$, $p=0.0529$) compared to WT virgins, which indicates fewer nurturing behaviors such as licking, carrying, and crouching and more harmful behaviors such as kicking, biting, and neglect. Furthermore, Bdnf-e1 -/- virgins displayed a reduced retrieval index compared to WT (**Fig. 1o**; Mann Whitney, $U = 31$, $p=0.0144$) indicative of a failure to bring pups to the existing nest or generate a new nest around foreign pups. Finally, a significant proportion of Bdnf-e1 -/- virgins showed decreased parenting compared to WT virgins (**Fig. 1p**; Mann-Whitney-Wilcoxon rank sum test, $W=39.5$, Bonferroni corrected $p= 0.0285$). This decrease in parenting behavior was accompanied by a substantial increase in

non-parenting (avoiding pups) as well as biting attacks. Interestingly, while *Bdnf-e1 -/-* postpartum mothers never showed aggression towards their biological offspring, *Bdnf-e1 -/-* virgins often attacked foreign pups (**Fig. 1p**).

Not only did *Bdnf-e1 -/-* females show impairments in maternal care, but they also showed perturbations in copulation behavior suggesting reduced mating receptivity (**Fig. S1**). It was difficult to impregnate pregnant *Bdnf-e1 -/-* females as male studs paired with these animals frequently showed a variety of genitalia injuries not commonly observed in WT breeder cages (**Fig. S1a-d**). In particular, there was a significant increase in the percentage of WT male breeders with injured genitalia when paired with heterozygous or homozygous *Bdnf-e1* females compared to WT females (**Fig. S1e**). To test whether male genitalia injuries were due to altered sexual behavior sequences or reduced female receptivity, we paired WT or *Bdnf-e1 -/-* estrous females with CD1 males and observed mating behavior. While WT and *Bdnf-e1 -/-* estrous females spent equal time exploring the cage (**Fig. S1f**), *Bdnf-e1 -/-* females were chased or cornered significantly more than WT females (**Fig. S1g**; Student's t-test, $t=2.147$, $df=22$, $p=0.0431$). *Bdnf-e1 -/-* females also showed a significant increase in the number of mounting rejections compared to WT females (**Fig. S1h**; Student's t-test, $t=2.932$, $df=22$, $p=0.0077$). Changes in mating behavior were not due to altered hormonal cycling as *Bdnf-e1 -/-* females entered estrous as determined by cytological evaluation (McLean, Valenzuela, Fai, & Bennett, 2012) ~every 5 days for at least 24 hours (**Fig. S2**). Furthermore, there were no instances of females attacking male genitalia (data not shown), suggesting that male injuries were likely due to altered copulation patterns and failure of females to enter lordosis. These results demonstrate that *Bdnf-e1 -/-* females have significant impairments in mating behavior associated with subsequent deficits in maternal care.

Disruption of BDNF-TrkB signaling in OXT neurons leads to reduced maternal care

Bdnf-e1 and *-e2 -/-* mice show significant loss of BDNF protein in the hypothalamus

(Maynard et al., 2016), a region containing key neuronal populations, such as oxytocin (OXT) neurons, critical for regulating social behaviors. Given the well-established role of OXT in regulating maternal behavior, we examined oxytocin (*Oxt*) and oxytocin receptor (*Oxtr*) transcript levels in *Bdnf*-e1, -e2, -e4, and -e6 *-/-* mice (**Fig. 2a-b**). Unlike *Bdnf*-e1 and -e2 *-/-* mice, *Bdnf*-e4 and -e6 *-/-* males do not show abnormal social behavior and *Bdnf*-e4 and -e6 *-/-* females breed successfully with no difficulties in pup survival (Maynard et al., 2016). Quantitative PCR revealed that *Bdnf*-e1 and -e2 *-/-* females show a 50% reduction of *Oxt* transcripts at postnatal day 28 compared to WT females (**Fig. 2a**; $F_{4,15} = 3.249$, $p = 0.0416$). Reductions in *Oxt* transcripts were unique to *Bdnf*-e1 and -e2 *-/-* mice and were not observed in *Bdnf*-e4 and -e6 *-/-* females. Downregulation of *Oxt* transcripts in *Bdnf*-e1 *-/-* females was specific to development as adult mutants showed normal *Oxt* transcript levels compared to WT ($t = 1.516$, $p > 0.05$). There were also no significant differences in hypothalamic *Oxtr* transcript levels between *Bdnf* mutants compared to WT (**Fig. 2b**). To characterize the oxytocinergic system, we quantified the number of OXT-expressing cells in the PVN of WT and *Bdnf*-1 *-/-* postpartum mothers (**Fig. 2c, f, i-k**). We found there were no significant differences in the size of the PVN (**Fig. 2i**), total number of PVN cells (**Fig. 2j**), or percentage of neurons expressing OXT (**Fig. 2k**). Given that OXT neurons are engaged by pup exposure and retrieval (Okabe et al., 2017), we next determined whether *Bdnf*-e1 *-/-* females show changes in OXT neuron activation during displays of maternal behavior. We immunolabeled neurons for OXT and cFOS, a surrogate marker for activated neurons, in the PVN of WT and *Bdnf*-e1 *-/-* postpartum mothers two hours following pup retrieval testing (**Fig. 2d, e, g, h**). We found no significant change in the percentage of OXT neurons labeled with cFOS (**Fig. 2l**), suggesting that OXT neurons are equally recruited during pup retrieval in WT and *Bdnf*-e1 *-/-* postpartum mothers.

The receptor for BDNF, tropomyosin receptor kinase B (TrkB), is highly expressed in OXT neurons (**Fig. 3a**), suggesting that BDNF may directly modulate OXT neuron function. To evaluate whether loss of BDNF signaling in OXT neurons contributes to impairments in maternal

care, we ablated TrkB selectively in OXT-expressing neurons by crossing mice expressing Cre-recombinase under control of the endogenous *Oxt* promoter (*Oxt^{Cre}*) to mice expressing a floxed TrkB allele (*TrkB^{flox/flox}*; **Fig. 3b**). Unlike *Bdnf-e1 -/-* postpartum mothers, *Oxt^{Cre}; TrkB^{flox/flox}* postpartum mothers with selective deletion of TrkB in OXT neurons showed normal pup survival compared to control mice (**Fig. 3c**). However, similar to *Bdnf-e1 -/-* mothers, *Oxt^{Cre}; TrkB^{flox/flox}* mothers showed a significant increase in latency to first pup retrieval (**Fig. 3d**; $t=2.297$, $df=25$, $p=0.0303$) and a strong trend for increased incidences of moving away from pups without retrieving (**Fig. 3e**). While analysis of global parenting style did not reveal significant reductions in parenting compared to control, a substantial proportion of *Oxt^{Cre}; TrkB^{flox/flox}* mothers were “non-parenters” and failed to engage with relocated pups (**Fig. 3f**). While *Oxt^{Cre}; TrkB^{flox/flox}* virgin females did not attack foreign pups as observed with *Bdnf-e1 -/-* virgins, a significant percentage of *Oxt^{Cre}; TrkB^{flox/flox}* virgins failed to parent (**Fig. 3h**; Mann-Whitney-Wilcoxon rank sum test, $W=21.5$, corrected $p=0.04236$) and showed trends for reduced nurturing behavior (**Fig. 3g**). Interestingly, *Oxt^{Cre}; TrkB^{flox/flox}* females showed no evidence of mating abnormalities and male breeders paired with these females did not sustain genitalia injuries. These results suggest that direct loss of BDNF-TrkB signaling in OXT neurons leads to altered maternal behavior.

Translatome profiling of OXT neurons in sexually mature females

Magnocellular and parvocellular neurons that release OXT are highly plastic in response to prolonged activation (Theodosios, 2002). However, the mechanisms underlying OXT neuron plasticity are not fully understood due to limited knowledge regarding the molecular identity of OXT neurons, which has been difficult to characterize due to the intermingled distribution of this population within the hypothalamus, particularly the paraventricular and supraoptic nuclei. To address this challenge and gain mechanistic detail into how BDNF-TrkB signaling might be impacting OXT neuron function and plasticity to modulate female-typical social behaviors, we

used translating ribosome affinity purification (TRAP) followed by RNA sequencing (RNA-seq) to characterize actively translating RNAs in hypothalamic neurons expressing OXT. We began by crossing *Oxt*^{Cre} mice to a Cre-dependent ribosome-tagged mouse (RiboTag mouse, referred to as *Rpl22*^{HA}) to allow for HA-tagging of ribosomes under control of the endogenous *Oxt* promoter (**Fig. 4a**). Ribosomes tagged selectively in OXT neurons were immunoprecipitated (IP) from total hypothalamic homogenate (Input) using an anti-HA antibody. Actively translating mRNAs were isolated from IP fractions and total mRNA was isolated from Input fractions.

Cell type-specific expression of the RiboTag allele in OXT neurons was confirmed by qPCR analysis showing significant enrichment (>100 fold) of *Oxt* expression in IP compared to Input (**Fig. 4b**). Following RNA amplification and library construction, we performed high-throughput RNA-seq on Input and IP RNA fractions to generate a comprehensive molecular profile of genes enriched and depleted in OXT neurons. Among the 22,472 expressed genes (at RPKM > 0.1), we identified 1,670 differentially expressed between Input and IP RNA fractions at FDR < 1%, including 1,129 genes with fold changes greater than 2 (**Table S1, Fig. 4c**). Differential analysis confirmed significant enrichment (IP/Input) of *Oxt* transcripts (59-fold increase, $t=16.6$, $p=2.94 \times 10^{-11}$) and significant depletion of transcripts for *Agrp*, *Cartpt*, and *Pmch* (3.8, 3.6, and 4.2 fold decreases, $p_{\text{adj}} = 0.015$, 8.88×10^{-5} , and 2.31×10^{-5} respectively), genes enriched in other hypothalamic nuclei, including the arcuate and lateral hypothalamus, respectively. A table of all genes expressed in *Oxt* IP RNA regardless of enrichment or depletion compared to total hypothalamic homogenate is found in **Table S2**. This list includes *Bdnf* and *Ntrk2*, the gene encoding TrkB, which is highly expressed throughout the hypothalamus, including in OXT neurons.

To confirm that RNA amplification prior to library construction did not bias sequencing data, we also generated low input RNA-seq libraries directly from Input and IP RNA fractions using the Nugen Ovation SoLo RNA-seq System, which produces strand-specific, rRNA depleted libraries from 10pg-10ng of RNA. Replication of differentially expressed genes (DEGs)

using the SoLo kit was very high. Approximately 99% of FDR-significant genes from RNA amplified samples were in the same direction as those from SoLo libraries, of which 92% were marginally significant ($p < 0.05$) (**Fig. S3; Table S2**). To identify a “neuronal translation” signature of genes that are enriched on translating ribosomes in neurons independent of cell-type, we compared our Oxt Input and IP fractions to publicly available TRAP data from Ntsr1+ cortical layer VI neurons (Nectow et al., 2017) and Input and IP fractions obtained from cortistatin (Cst) inhibitory interneurons (**Table S2**). We identified 14 genes enriched on actively translating ribosomes in OXT neurons as well as in excitatory and inhibitory neurons (*Etl4*, *Kalrn*, *Actn4*, *Copa*, *Myo5b*, *Cdc42bpb*, *Phrf1*, *Gtf3c1*, *Srrm1*, *Nefm*, *Srcin1*, *Mapk8ip3*, *Fasn*, *Arhgef11*). All three cell types were de-enriched for a set of 50 genes, including *Apoe* and *Mog*, genes enriched in astrocytes and oligodendrocytes, respectively.

Highly enriched translating mRNA species in OXT neurons presumably represent the most functionally relevant genes for this cell type. To discover which classes of mRNAs are preferentially expressed in female OXT neurons, we performed gene ontology (GO) enrichment analysis on the subset of the 756 genes (with Entrez IDs) more highly expressed in Oxt neurons compared to total hypothalamic homogenate and also on the 813 Entrez genes more highly expressed in homogenate tissue (**Fig. 4d; Table S3**). Analysis with the cellular component category showed that OXT-enriched mRNAs encode proteins critical for structural plasticity, including cytoskeletal and postsynaptic organization. Analysis with the molecular function category revealed genes that encode signaling molecules critical for binding to actin, microtubules, GTPases, calmodulin, and syntaxin-1, suggesting robust expression of proteins that regulate synaptic structure and exocytosis in OXT neurons. Reassuringly, pathways relevant for gliogenesis, myelin, and oligodendrocyte differentiation contained genes more highly expressed in homogenate tissue compared to OXT neurons. Given the central role of oxytocin in regulating social behavior, we examined whether genes enriched in female OXT neurons (e.g. more highly expressed than homogenate tissue and $FDR < 1\%$) overlap with

genes implicated in autism spectrum disorder (ASD) by the Simons Foundation Autism Research Initiative (SFARI). We first found strong enrichment among the 224 genes with mouse Genetic Animal Models of ASD - 30 of these genes (13%, OR=4.24, $p=6.62e-10$) were significantly more highly expressed in OXT neurons than homogenate tissue (**Table S4**). We further found strong enrichment of genes in the SFARI Human Gene Module using the subset of mouse-expressed genes with human homologs (N=14,769) – 131 of the 842 expressed Human SFARI genes were enriched in OXT neurons (15.5%, OR=4.0, $p<2.2e-16$). (**Fig. 4e; Table S5**). Many of these genes encode proteins that modulate synaptic function and plasticity, suggesting a link between OXT neuron adaptability and social behavior.

Disruption of BDNF alters gene expression in OXT neurons

To delineate how perturbations in BDNF signaling impact OXT-enriched genes to modulate female-typical social behavior, we next compared the transcriptome of OXT neurons in control versus *Bdnf-e1* mutant mice. Due to difficulties in obtaining *Bdnf-e1*; *Oxt*^{Cre}; *Rpl22*^{HA} triple crossed mice (*Bdnf* and *Oxt* are both located on chromosome 2 resulting in infrequent recombination of the mutant allele with the Cre transgene and RiboTag reporter), we switched to a viral strategy and sought to optimize expression profiling in OXT neurons from individual, instead of pooled, samples. We generated *Bdnf-e1*; *Oxt*^{Cre}; tdTom mice and utilized an adeno-associated virus (AAV) that initiates Cre-inducible RiboTag expression using a double floxed inverted open reading frame (DIO) approach (Sanz et al., 2015) (**Fig. 5a**). Viral delivery into the PVN (**Fig. 5b**) had two additional advantages: 1) it ensured profiling of neurons that were actively utilizing the *Oxt* promoter in adulthood and 2) it allowed for targeting of OXT populations selectively in the PVN as opposed to the supraoptic nucleus (SON). We isolated IP RNA from control (*Bdnf-e1* +/+; *Oxt*^{Cre}; tdTom) and mutant (*Bdnf-e1* -/-; *Oxt*^{Cre}; tdTom) virgin female mice infused with AAV-DIO-Ribotag and directly generated RNA-seq libraries from each individual mouse using the Nugen Ovation SoLo RNA-seq System.

Differential expression analysis accounting for sample variation and differences in

transfection or enrichment efficiency (via exonic mapping rate and *Oxt* expression itself) revealed 100 differentially expressed genes between control IP vs. *Bdnf-e1* ^{-/-} IP samples at FDR < 10% which was controlled by $p < 0.00038$. (**Fig. 5c; Table S6**). Importantly, DEGs between *Oxt* IP vs. *Oxt* Input in WT females did not overlap with DEGs between control IP and *Bdnf-e1* ^{-/-} IP samples, suggesting efficient immunoprecipitation of ribosomes in OXT neurons. (**Fig. S4**). Of particular interest, we identified significant elevation in *Gabra2*, a subunit for the GABA_A receptor, which is known to mediate inhibition onto OXT neurons and shows expression modulation through BDNF signaling (Choe et al., 2015; Hewitt & Bains, 2006). Furthermore, *Bdnf-e1* ^{-/-} OXT neurons exhibited downregulation of *Cckar*, a gene encoding the cholecystokinin A receptor, which is critical for female mating behavior (X. Xu et al., 2012). Changes in the levels of *Gabra2* and *Cckar* between control and *Bdnf-e1* ^{-/-} OXT neurons were validated by fluorescent *in situ* hybridization using RNAscope (**Fig. 5e, f**). Unexpectedly, a number of the differentially expressed genes in OXT neurons between control and *Bdnf-e1* ^{-/-} were mitochondrial genes, suggesting that BDNF disruption leads to dysregulation in oxidative phosphorylation systems that mediate cellular energy and metabolism. This is consistent with previous literature demonstrating a neuroprotective role for BDNF in mitigating metabolic defects and promoting cellular stress resistance during plasticity (Raefsky & Mattson, 2017; Z. Xu, Lv, Dai, Lu, & Jin, 2017).

GO analysis with the biological process, molecular function, and cellular component categories identified gene sets significantly different between control and *Bdnf-e1* ^{-/-} OXT neurons as encoding proteins that are known to function at synapses, axons, and the respiratory chain in mitochondria (**Fig. 5d; Table S7**). For example, GO terms significantly different in the molecular function category included NADH (nicotinamide adenine dinucleotide) dehydrogenase activity, transmembrane receptor protein tyrosine kinase activity, and neuropeptide hormone activity (**Fig. 5d**). Differentially expressed gene sets between control and *Bdnf-e1* ^{-/-} OXT neurons were also enriched in development-related GO terms for biological

processes such as axon development, neuronal differentiation and migration, and synaptic assembly and transmission (**Table S7**). We also examined whether DEGs between control and *Bdnf-e1* ^{-/-} OXT neurons overlap with SFARI genes implicated in ASD. Here we found significant enrichment with the Genetic Animal Model ASD genes, specifically *Reln*, *Nrp2*, *ErbB4*, *Gad1*, and *Pou3f2*, with those genes dysregulated in OXT neurons following disruption of BDNF signaling ($p=0.0036$, OR=5.21, **Table S8**) with only suggestive enrichment of the more general Human SFARI ASD genes ($p=0.067$, OR=2.0) which contains the above five mouse model genes plus *Avp* and *Chrm3*. Taken together, these results suggest that perturbations in hypothalamic BDNF-TrkB signaling lead to dysregulation of plasticity mechanisms in OXT neurons that may impact female social behavior.

Discussion:

While a casual role for BDNF in regulating male-typical social behaviors has been well-established, the contribution of BDNF signaling to female-typical social behaviors has remained unexplored. Here we demonstrate a novel role for BDNF in modulating maternal care and sexual receptivity in female mice. Furthermore, we provide evidence that BDNF-TrkB signaling in hypothalamic OXT neurons contributes to maternal behavior. We define a molecular profile for OXT neurons and delineate how perturbations in BDNF-TrkB signaling impact gene expression in OXT neurons to influence female-typical social behaviors. Our studies identify hypothalamic BDNF as a broad modulator of sex-specific social behaviors and elucidate new activity-dependent synaptic plasticity pathways critical for OXT neuron function.

BDNF impacts female-typical social behaviors

The majority of literature surrounding BDNF in the context of maternal care has focused on offspring. A large body of work has demonstrated that increased prenatal stress or reduced maternal care leads to downregulation of BDNF in developing offspring and subsequent deficits in adult behavior (Branchi et al., 2013; Cirulli et al., 2009; Hill, Warren, & Roth, 2014). However,

no studies have investigated the reverse relationship to ask whether BDNF levels in mothers play a causal role in regulating displays of maternal behavior. This is especially surprising given that BDNF is well-established as a robust modulator of male-typical social behavior, particularly aggression. Heterozygous mice with a 50% reduction of global BDNF show enhanced aggression and alterations in serotonin signaling (Lyons et al., 1999). Furthermore, we have previously shown that selective disruption of BDNF from promoters I or II, but not IV or VI, leads to significant loss of BDNF in the hypothalamus and elevated aggression and mounting behavior during fighting (Maynard et al., 2016). Gaps in understanding how BDNF controls female social behavior are also surprising given that estrogen robustly increases BDNF expression and impacts dendritic spine plasticity to modulate behaviors such as cognition (Luine & Frankfurt, 2013). These studies suggest important sexually dimorphic effects of BDNF on neural circuitry and behavior that have been relatively unexplored.

Akin to social deficits in *Bdnf-e1* and *-e2 -/-* males, we find that selective disruption of promoter I and II-derived BDNF in females leads to significant impairments in sex-typical social behaviors, including pup retrieval and mating behavior. While WT postpartum females exhibit stereotyped patterns of maternal care in which they systematically retrieve and nurture pups (Lonstein & De Vries, 2000), *Bdnf-e1* and *-e2 -/-* dams show disorganized parenting behavior and decreased pup survival. Furthermore, unlike WT virgins that show affiliative behaviors towards foreign pups (Svare & Mann, 1981), *Bdnf-e1 -/-* virgins find foreign pups aversive and ignore or attack them. *Bdnf-e1 -/-* females also display reduced sexual receptivity towards WT males resulting in male genitalia injuries, disrupted mating patterns, and decreased probability of conception. Similar to *Bdnf-e1* and *Bdnf-e2 -/-* males, *Bdnf-e1* and *-e2 -/-* females show differences in phenotype severity with *Bdnf-e1 -/-* females having stronger phenotypes. For example, *Bdnf-e1 -/-* postpartum females exhibit greater pup loss compared to *Bdnf-e2 -/-* postpartum females. We speculate that decreased pup survival for *Bdnf-e1 -/-* dams may result from a combination of parental neglect, infanticide, and inconsistencies in nursing behavior.

Future experiments should distinguish between these possibilities and explore the role of BDNF-TrkB signaling in regulation of lactation, which is modulated by neuropeptides such as oxytocin (Nishimori et al., 1996). Given that promoter I is more highly sensitive to neural activity than promoter II (Timmusk et al., 1993), it is possible that phenotype severity in *Bdnf-e1* $-/-$ females may be accounted for by loss of activity-induced BDNF that is critical for synaptic plasticity. Furthermore, *Bdnf-e2* $-/-$ mice show compensatory downregulation of *Bdnf* exon I transcripts (Maynard et al., 2016), which may drive their exhibited deficits in maternal care.

Relationship between BDNF signaling, oxytocin, and maternal behavior

Bdnf-e1 and *-e2* mutants show a 50% reduction of BDNF protein in the hypothalamus, suggesting that promoters I and II are heavily used in this brain region (Maynard et al., 2016). BDNF and its receptor TrkB are highly expressed in several hypothalamic nuclei, including the paraventricular nucleus, a primary site of magnocellular and parvocellular neurons that secrete oxytocin (Dolen, 2015; Smith, Makino, Kim, & Kvetnansky, 1995). Oxytocin is a neuropeptide with well-established roles in modulating sex-typical social behaviors, including maternal behaviors such as pup retrieval (Marlin et al., 2015; Pedersen, Ascher, Monroe, & Prange, 1982). We find that disruption of BDNF production from promoters I and II leads to transient decreases in *Oxt* gene expression in *Bdnf-e1* and *-e2* $-/-$ females before sexual maturity. Early dysregulations in *Oxt* expression may be indicative of developmental impairments in the oxytocinergic system that contribute to mating and parenting deficits in adult females. Indeed, manipulating levels of OXT during early postnatal development has long-lasting effects on social behaviors into adulthood (Bales & Carter, 2003; Penagarikano et al., 2015; Yamamoto et al., 2004). Interestingly, sexually mature *Bdnf-e1* $-/-$ females show normal *Oxt* expression compared to WT and do not exhibit deficits in the number or activation of OXT neurons during pup retrieval. These findings suggest that BDNF may not regulate OXT neuron survival or recruitment, but may instead have more subtle effects on synaptic plasticity or gene regulation in OXT neurons. Our molecular profiling data support this hypothesis and provide evidence that

BDNF may modulate the morphology and activity of OXT neurons to influence the location and timing of OXT release.

Importantly, loss of TrkB in OXT neurons partially recapitulates maternal care deficits in *Bdnf-e1 -/-* females, suggesting that BDNF-TrkB signaling in OXT neurons is sufficient to modulate female-typical social behavior. However, as phenotypes in *Oxt^{Cre}; TrkB^{flox/flox}* females were milder than those observed in *Bdnf-e1 -/-* females, it is likely that BDNF-TrkB signaling in other hypothalamic populations associated with parental behavior, such as the medial preoptic area (MPO) and anteroventral periventricular nucleus (AVPV) (Scott, Prigge, Yizhar, & Kimchi, 2015; Wu, Autry, Bergan, Watabe-Uchida, & Dulac, 2014), contribute to the regulation of female-typical social behaviors. Indeed, a monosynaptic circuit linking dopamine neurons in the periventricular hypothalamus to OXT neurons in the PVN was recently identified and shown to control OXT neuron secretion and maternal care (Scott et al., 2015). As BDNF plays an important role in the survival and function of dopamine neurons (Altar et al., 1992; Hyman et al., 1991; Lobo et al., 2010; Loudes, Petit, Kordon, & Faivre-Bauman, 1999), future studies should investigate whether BDNF-TrkB signaling also acts in this circuit to impact female-typical social behaviors.

Molecular profile for OXT neurons in sexually mature females

Establishing a molecular profile for OXT neurons has been hindered by the intermingled distribution of this population within the hypothalamus, which poses a significant challenge for achieving cell-type specific gene expression. Over a decade ago, single-cell RT-PCR was used to identify cell-specific mRNAs expressed in magnocellular neurons selectively expressing oxytocin or vasopressin (Yamashita et al., 2002). While the authors identified 48 previously unknown genes to be expressed in magnocellular neurons in the lactating rat, the microarray approach did not allow for characterization of global gene expression. Using a translating ribosome affinity purification approach combined with RNA-sequencing, we identified ~1700 actively translated genes differentially expressed in OXT neurons compared to total

hypothalamic homogenate, including ~1000 genes with a greater than 2-fold change in either direction. Gene ontology analysis revealed that many OXT-enriched genes encode proteins critical for structural and functional plasticity that act in pathways modulating synaptic and cytoskeletal organization as well as calmodulin and actin binding. As OXT neurons show remarkable morphological, electrophysiological, and synaptic remodeling in response to environmental events such as parturition and lactation (Theodosis, 2002), our results suggest a dynamic gene transcription program that supports rapid activity-induced, experience-dependent plasticity. Interestingly, we also saw enrichment of paternally-expressed gene 3, or *Peg3*, an imprinted gene that is expressed exclusively from the paternal allele and regulates maternal behavior (L. Li et al., 1999). Future studies should identify the molecular profile of OXT neurons in males to determine sexually dimorphic gene expression that may underlie male and female-typical social behaviors.

Identification of a molecular profile for OXT neurons may provide new insights into how the oxytocin system can be modulated to improve social behavior, especially in the context of autism spectrum disorder (ASD), which is characterized by deficits in social communication and interaction. Indeed, we find that differentially expressed genes in OXT neurons overlap with both mouse and human genes that have been implicated in ASD by the Simons Foundation Autism Research Initiative. Many of these genes encode proteins that are critical for structural and functional plasticity and could represent novel targets for enhancing OXT release. Given that OXT is of great interest for therapeutic intervention but does not easily cross the blood brain barrier (Landgraf, Ermisch, & Hess, 1979; McEwen, 2004), the molecular profile of OXT neurons presented here provides a valuable resource for probing gene pathways critical for OXT expression and regulation. One limitation of our study is that we do not distinguish between magnocellular and parvocellular neurons, which have different neuronal projections and functions (Dolen, 2015). While it is likely that OXT neurons can be classified into at least four different subtypes (Althammer & Grinevich, 2017; Romanov et al., 2017), future

experiments using retrograde expression of the RiboTag allele to label specific OXT projections may begin to parse out molecular profiles for functionally distinct classes of OXT neurons.

BDNF modulates plasticity genes in OXT neurons

BDNF is a robust modulator of activity-dependent gene expression and synaptic plasticity (Berton et al., 2006; Lu, 2003). To determine how perturbations in BDNF signaling impact OXT-enriched genes to potentially influence female-typical social behaviors, we compared the transcriptomes of OXT neurons from control and *Bdnf-e1* ^{-/-} mice. We found ~100 genes differentially expressed in OXT neurons following disruption of promoter I-derived BDNF. Differentially expressed genes in *Bdnf-e1* ^{-/-} OXT neurons were enriched in pathways critical for morphological and synaptic plasticity. Gene ontology analysis revealed that many of these genes encode proteins that function in mitochondrial pathways important for cellular energy and adaptive responses to neural activity. This is consistent with previous reports showing that BDNF stimulates mitochondrial biogenesis in hippocampal neurons (Cheng et al., 2012) and can enhance synaptic transmission by arresting mitochondria at active synapses to fuel dendritic spine dynamics and synaptic plasticity (Z. Li, Okamoto, Hayashi, & Sheng, 2004; Raefsky & Mattson, 2017; Su, Ji, Sun, Liu, & Chen, 2014).

We also found significant elevation of *Gabra2*, a gene encoding a subunit for the GABA_A receptor. Plasticity at inhibitory synapses is strongly modulated by expression, localization, and function of GABA_A receptors (Mele, Leal, & Duarte, 2016), which mediate inhibition onto magnocellular and parvocellular neurons and play a key role in their adaptive responses following stimulation (Bali & Kovacs, 2003; Lee et al., 2015). Elevation of *Gabra2* following loss of BDNF signaling is consistent with previous reports demonstrating that BDNF is a robust modulator of synaptic inhibition and GABA_A receptors (Brunig, Penschuck, Berninger, Benson, & Fritschy, 2001; Jovanovic, Thomas, Kittler, Smart, & Moss, 2004; Tanaka, Saito, & Matsuki, 1997) and can reduce inhibitory synaptic drive on neuroendocrine cells by decreasing GABA_A surface expression (Hewitt & Bains, 2006). BDNF has also been shown to decrease inhibition

of vasopressin neurons through downregulation of GABA_A receptor signaling (Choe et al., 2015). Taken together, these findings suggest that disruption of hypothalamic BDNF may lead to increased inhibition onto OXT neurons that could alter the timing or levels of OXT release to impact social behaviors. Interestingly, we also saw substantial downregulation of *Cckar*, a gene encoding the cholecystokinin A receptor. While *Cckar* is associated with feeding and metabolism (Baile, Della-Fera, & McLaughlin, 1983), it is also essential for sexual receptivity in females (X. Xu et al., 2012). Similar to *Bdnf-e1* ^{-/-} females, *Cckar* null females show reduced sexual receptivity, suggesting that BDNF and cholecystokinin signaling may interact in OXT neurons to control female sexual behavior. As estrogen induces both *Bdnf* and *Cckar* expression (Luine & Frankfurt, 2013; X. Xu et al., 2012), this may point to a sexually-dimorphic pathway in OXT neurons that influences female-specific social behaviors.

In conclusion, we demonstrate that BDNF-TrkB signaling in oxytocin neurons, and likely additional hypothalamic populations, plays a causal role in modulating female-typical social behavior. We identify OXT neurons as enriched in genes important for structural and functional plasticity, and show that perturbations in BDNF signaling lead to disruption of OXT neuron gene expression that may impact maternal behavior in females.

Acknowledgements

We thank Dr. Harold Gainer (NIH, Bethesda) for generously providing the OXT antibody. We thank Dr. Stanley McKnight (University of Washington, Seattle) for the generous gift of AAV-DIO-Ribotag vector. We acknowledge the Penn Vector Core (University of Pennsylvania, Philadelphia) for viral packaging. We thank Dr. Daniel Weinberger for comments on the manuscript. Funding for these studies was provided by the Lieber Institute for Brain Development and the National Institute for Mental Health (T32MH01533037 to KRM and RO1MH105592 to KM).

References

- Aid, T., Kazantseva, A., Piirsoo, M., Palm, K., & Timmusk, T. (2007). Mouse and rat BDNF gene structure and expression revisited. *J Neurosci Res*, 85(3), 525-535.
doi:10.1002/jnr.21139
- Altar, C. A., Boylan, C. B., Jackson, C., Hershenson, S., Miller, J., Wiegand, S. J., . . . Hyman, C. (1992). Brain-derived neurotrophic factor augments rotational behavior and nigrostriatal dopamine turnover in vivo. *Proc Natl Acad Sci U S A*, 89(23), 11347-11351.
- Althammer, F., & Grinevich, V. (2017). Diversity of oxytocin neurons: beyond magno- and parvocellular cell types? *J Neuroendocrinol*. doi:10.1111/jne.12549
- Andero, R., Choi, D. C., & Ressler, K. J. (2014). BDNF-TrkB receptor regulation of distributed adult neural plasticity, memory formation, and psychiatric disorders. *Prog Mol Biol Transl Sci*, 122, 169-192. doi:10.1016/B978-0-12-420170-5.00006-4
- Baile, C. A., Della-Fera, M. A., & McLaughlin, C. L. (1983). Hormones and feed intake. *Proc Nutr Soc*, 42(2), 113-127.
- Baj, G., D'Alessandro, V., Musazzi, L., Mallei, A., Sartori, C. R., Sciancalepore, M., . . . Tongiorgi, E. (2012). Physical exercise and antidepressants enhance BDNF targeting in hippocampal CA3 dendrites: further evidence of a spatial code for BDNF splice variants. *Neuropsychopharmacology*, 37(7), 1600-1611. doi:10.1038/npp.2012.5
- Baj, G., Leone, E., Chao, M. V., & Tongiorgi, E. (2011). Spatial segregation of BDNF transcripts enables BDNF to differentially shape distinct dendritic compartments. *Proc Natl Acad Sci U S A*, 108(40), 16813-16818. doi:10.1073/pnas.1014168108
- Bales, K. L., & Carter, C. S. (2003). Developmental exposure to oxytocin facilitates partner preferences in male prairie voles (*Microtus ochrogaster*). *Behav Neurosci*, 117(4), 854-859.

- Bali, B., & Kovacs, K. J. (2003). GABAergic control of neuropeptide gene expression in parvocellular neurons of the hypothalamic paraventricular nucleus. *Eur J Neurosci*, 18(6), 1518-1526.
- Ben-Barak, Y., Russell, J. T., Whitnall, M. H., Ozato, K., & Gainer, H. (1985). Neurophysin in the hypothalamo-neurohypophyseal system. I. Production and characterization of monoclonal antibodies. *J Neurosci*, 5(1), 81-97.
- Berton, O., McClung, C. A., Dileone, R. J., Krishnan, V., Renthal, W., Russo, S. J., . . . Nestler, E. J. (2006). Essential role of BDNF in the mesolimbic dopamine pathway in social defeat stress. *Science*, 311(5762), 864-868. doi:10.1126/science.1120972
- Branchi, I., Curley, J. P., D'Andrea, I., Cirulli, F., Champagne, F. A., & Alleva, E. (2013). Early interactions with mother and peers independently build adult social skills and shape BDNF and oxytocin receptor brain levels. *Psychoneuroendocrinology*, 38(4), 522-532. doi:10.1016/j.psyneuen.2012.07.010
- Brunig, I., Penschuck, S., Berninger, B., Benson, J., & Fritschy, J. M. (2001). BDNF reduces miniature inhibitory postsynaptic currents by rapid downregulation of GABA(A) receptor surface expression. *Eur J Neurosci*, 13(7), 1320-1328.
- Carlier, M., Roubertoux, P., & Cohen-Salmon, C. (1982). Differences in patterns of pup care in *Mus musculus domesticus* I-Comparisons between eleven inbred strains. *Behav Neural Biol*, 35(2), 205-210.
- Chan, J. P., Unger, T. J., Byrnes, J., & Rios, M. (2006). Examination of behavioral deficits triggered by targeting Bdnf in fetal or postnatal brains of mice. *Neuroscience*, 142(1), 49-58. doi:10.1016/j.neuroscience.2006.06.002
- Chao, M. V., Rajagopal, R., & Lee, F. S. (2006). Neurotrophin signalling in health and disease. *Clin Sci (Lond)*, 110(2), 167-173. doi:10.1042/CS20050163

- Cheng, A., Wan, R., Yang, J. L., Kamimura, N., Son, T. G., Ouyang, X., . . . Mattson, M. P. (2012). Involvement of PGC-1alpha in the formation and maintenance of neuronal dendritic spines. *Nat Commun*, 3, 1250. doi:10.1038/ncomms2238
- Choe, K. Y., Han, S. Y., Gaub, P., Shell, B., Voisin, D. L., Knapp, B. A., . . . Bourque, C. W. (2015). High salt intake increases blood pressure via BDNF-mediated downregulation of KCC2 and impaired baroreflex inhibition of vasopressin neurons. *Neuron*, 85(3), 549-560. doi:10.1016/j.neuron.2014.12.048
- Cirulli, F., Francia, N., Berry, A., Aloe, L., Alleva, E., & Suomi, S. J. (2009). Early life stress as a risk factor for mental health: role of neurotrophins from rodents to non-human primates. *Neurosci Biobehav Rev*, 33(4), 573-585. doi:10.1016/j.neubiorev.2008.09.001
- Dolen, G. (2015). Oxytocin: parallel processing in the social brain? *J Neuroendocrinol*, 27(6), 516-535. doi:10.1111/jne.12284
- Grishanin, R. N., Yang, H., Liu, X., Donohue-Rolfe, K., Nune, G. C., Zang, K., . . . Reichardt, L. F. (2008). Retinal TrkB receptors regulate neural development in the inner, but not outer, retina. *Mol Cell Neurosci*, 38(3), 431-443. doi:10.1016/j.mcn.2008.04.004
- Hewitt, S. A., & Bains, J. S. (2006). Brain-derived neurotrophic factor silences GABA synapses onto hypothalamic neuroendocrine cells through a postsynaptic dynamin-mediated mechanism. *J Neurophysiol*, 95(4), 2193-2198. doi:10.1152/jn.01135.2005
- Hill, K. T., Warren, M., & Roth, T. L. (2014). The influence of infant-caregiver experiences on amygdala Bdnf, OXTr, and NPY expression in developing and adult male and female rats. *Behav Brain Res*, 272, 175-180. doi:10.1016/j.bbr.2014.07.001
- Hodneland, E., Kogel, T., Frei, D. M., Gerdes, H. H., & Lundervold, A. (2013). CellSegm - a MATLAB toolbox for high-throughput 3D cell segmentation. *Source Code Biol Med*, 8(1), 16. doi:10.1186/1751-0473-8-16

- Hyman, C., Hofer, M., Barde, Y. A., Juhasz, M., Yancopoulos, G. D., Squinto, S. P., & Lindsay, R. M. (1991). BDNF is a neurotrophic factor for dopaminergic neurons of the substantia nigra. *Nature*, 350(6315), 230-232. doi:10.1038/350230a0
- Ito, W., Chehab, M., Thakur, S., Li, J., & Morozov, A. (2011). BDNF-restricted knockout mice as an animal model for aggression. *Genes Brain Behav*, 10(3), 365-374. doi:10.1111/j.1601-183X.2010.00676.x
- Jaffe, A. E., Tao, R., Norris, A. L., Kealhofer, M., Nellore, A., Shin, J. H., . . . Weinberger, D. R. (2017). qSVA framework for RNA quality correction in differential expression analysis. *Proc Natl Acad Sci U S A*, 114(27), 7130-7135. doi:10.1073/pnas.1617384114
- Jovanovic, J. N., Thomas, P., Kittler, J. T., Smart, T. G., & Moss, S. J. (2004). Brain-derived neurotrophic factor modulates fast synaptic inhibition by regulating GABA(A) receptor phosphorylation, activity, and cell-surface stability. *J Neurosci*, 24(2), 522-530. doi:10.1523/JNEUROSCI.3606-03.2004
- Kasen, S., Ouellette, R., & Cohen, P. (1990). Mainstreaming and postsecondary educational and employment status of a rubella cohort. *Am Ann Deaf*, 135(1), 22-26.
- Kim, D., Langmead, B., & Salzberg, S. L. (2015). HISAT: a fast spliced aligner with low memory requirements. *Nat Methods*, 12(4), 357-360. doi:10.1038/nmeth.3317
- Kusano, K., House, S. B., & Gainer, H. (1999). Effects of osmotic pressure and brain-derived neurotrophic factor on the survival of postnatal hypothalamic oxytocinergic and vasopressinergic neurons in dissociated cell culture. *J Neuroendocrinol*, 11(2), 145-152.
- Landgraf, R., Ermisch, A., & Hess, J. (1979). Indications for a brain uptake of labelled vasopressin and oxytocin and the problem of the blood-brain barrier. *Endokrinologie*, 73(1), 77-81.
- Law, C. W., Chen, Y., Shi, W., & Smyth, G. K. (2014). voom: Precision weights unlock linear model analysis tools for RNA-seq read counts. *Genome Biol*, 15(2), R29. doi:10.1186/gb-2014-15-2-r29

- Lee, S. W., Kim, Y. B., Kim, J. S., Kim, W. B., Kim, Y. S., Han, H. C., . . . In Kim, Y. (2015). GABAergic inhibition is weakened or converted into excitation in the oxytocin and vasopressin neurons of the lactating rat. *Mol Brain*, 8, 34. doi:10.1186/s13041-015-0123-0
- Li, L., Keverne, E. B., Aparicio, S. A., Ishino, F., Barton, S. C., & Surani, M. A. (1999). Regulation of maternal behavior and offspring growth by paternally expressed Peg3. *Science*, 284(5412), 330-333.
- Li, Z., Okamoto, K., Hayashi, Y., & Sheng, M. (2004). The importance of dendritic mitochondria in the morphogenesis and plasticity of spines and synapses. *Cell*, 119(6), 873-887. doi:10.1016/j.cell.2004.11.003
- Liao, Y., Smyth, G. K., & Shi, W. (2014). featureCounts: an efficient general purpose program for assigning sequence reads to genomic features. *Bioinformatics*, 30(7), 923-930. doi:10.1093/bioinformatics/btt656
- Liu, D., Diorio, J., Day, J. C., Francis, D. D., & Meaney, M. J. (2000). Maternal care, hippocampal synaptogenesis and cognitive development in rats. *Nat Neurosci*, 3(8), 799-806. doi:10.1038/77702
- Lobo, M. K., Covington, H. E., 3rd, Chaudhury, D., Friedman, A. K., Sun, H., Damez-Werno, D., . . . Nestler, E. J. (2010). Cell type-specific loss of BDNF signaling mimics optogenetic control of cocaine reward. *Science*, 330(6002), 385-390. doi:10.1126/science.1188472
- Lonstein, J. S., & De Vries, G. J. (2000). Sex differences in the parental behavior of rodents. *Neurosci Biobehav Rev*, 24(6), 669-686.
- Louides, C., Petit, F., Kordon, C., & Faivre-Bauman, A. (1999). Distinct populations of hypothalamic dopaminergic neurons exhibit differential responses to brain-derived neurotrophic factor (BDNF) and neurotrophin-3 (NT3). *Eur J Neurosci*, 11(2), 617-624.
- Lu, B. (2003). BDNF and activity-dependent synaptic modulation. *Learn Mem*, 10(2), 86-98. doi:10.1101/lm.54603

- Luine, V., & Frankfurt, M. (2013). Interactions between estradiol, BDNF and dendritic spines in promoting memory. *Neuroscience*, 239, 34-45. doi:10.1016/j.neuroscience.2012.10.019
- Lyons, W. E., Mamounas, L. A., Ricaurte, G. A., Coppola, V., Reid, S. W., Bora, S. H., . . . Tessarollo, L. (1999). Brain-derived neurotrophic factor-deficient mice develop aggressiveness and hyperphagia in conjunction with brain serotonergic abnormalities. *Proc Natl Acad Sci U S A*, 96(26), 15239-15244.
- Marlin, B. J., Mitre, M., D'Amour J, A., Chao, M. V., & Froemke, R. C. (2015). Oxytocin enables maternal behaviour by balancing cortical inhibition. *Nature*, 520(7548), 499-504. doi:10.1038/nature14402
- Maynard, K. R., Hill, J. L., Calcaterra, N. E., Palko, M. E., Kardian, A., Paredes, D., . . . Martinowich, K. (2016). Functional Role of BDNF Production from Unique Promoters in Aggression and Serotonin Signaling. *Neuropsychopharmacology*, 41(8), 1943-1955. doi:10.1038/npp.2015.349
- McEwen, B. B. (2004). Brain-fluid barriers: relevance for theoretical controversies regarding vasopressin and oxytocin memory research. *Adv Pharmacol*, 50, 531-592, 655-708. doi:10.1016/S1054-3589(04)50014-5
- McLean, A. C., Valenzuela, N., Fai, S., & Bennett, S. A. (2012). Performing vaginal lavage, crystal violet staining, and vaginal cytological evaluation for mouse estrous cycle staging identification. *J Vis Exp*(67), e4389. doi:10.3791/4389
- Mele, M., Leal, G., & Duarte, C. B. (2016). Role of GABAA R trafficking in the plasticity of inhibitory synapses. *J Neurochem*, 139(6), 997-1018. doi:10.1111/jnc.13742
- Moreno, G., Piermaria, J., Gaillard, R. C., & Spinedi, E. (2011). In vitro functionality of isolated embryonic hypothalamic vasopressinergic and oxytocinergic neurons: modulatory effects of brain-derived neurotrophic factor and angiotensin II. *Endocrine*, 39(1), 83-88. doi:10.1007/s12020-010-9415-4

- Nectow, A. R., Moya, M. V., Ekstrand, M. I., Mousa, A., McGuire, K. L., Sferrazza, C. E., . . . Schmidt, E. F. (2017). Rapid Molecular Profiling of Defined Cell Types Using Viral TRAP. *Cell Rep*, 19(3), 655-667. doi:10.1016/j.celrep.2017.03.048
- Neumann, I. D. (2008). Brain oxytocin: a key regulator of emotional and social behaviours in both females and males. *J Neuroendocrinol*, 20(6), 858-865. doi:10.1111/j.1365-2826.2008.01726.x
- Nishimori, K., Young, L. J., Guo, Q., Wang, Z., Insel, T. R., & Matzuk, M. M. (1996). Oxytocin is required for nursing but is not essential for parturition or reproductive behavior. *Proc Natl Acad Sci U S A*, 93(21), 11699-11704.
- Okabe, S., Tsuneoka, Y., Takahashi, A., Ooyama, R., Watarai, A., Maeda, S., . . . Kikusui, T. (2017). Pup exposure facilitates retrieving behavior via the oxytocin neural system in female mice. *Psychoneuroendocrinology*, 79, 20-30. doi:10.1016/j.psyneuen.2017.01.036
- Pattabiraman, P. P., Tropea, D., Chiaruttini, C., Tongiorgi, E., Cattaneo, A., & Domenici, L. (2005). Neuronal activity regulates the developmental expression and subcellular localization of cortical BDNF mRNA isoforms in vivo. *Mol Cell Neurosci*, 28(3), 556-570. doi:10.1016/j.mcn.2004.11.010
- Pedersen, C. A., Ascher, J. A., Monroe, Y. L., & Prange, A. J., Jr. (1982). Oxytocin induces maternal behavior in virgin female rats. *Science*, 216(4546), 648-650.
- Penagarikano, O., Lazaro, M. T., Lu, X. H., Gordon, A., Dong, H., Lam, H. A., . . . Geschwind, D. H. (2015). Exogenous and evoked oxytocin restores social behavior in the Cntnap2 mouse model of autism. *Sci Transl Med*, 7(271), 271ra278. doi:10.1126/scitranslmed.3010257
- Pruunsild, P., Kazantseva, A., Aid, T., Palm, K., & Timmusk, T. (2007). Dissecting the human BDNF locus: bidirectional transcription, complex splicing, and multiple promoters. *Genomics*, 90(3), 397-406. doi:10.1016/j.ygeno.2007.05.004

- Raefsky, S. M., & Mattson, M. P. (2017). Adaptive responses of neuronal mitochondria to bioenergetic challenges: Roles in neuroplasticity and disease resistance. *Free Radic Biol Med*, 102, 203-216. doi:10.1016/j.freeradbiomed.2016.11.045
- Ram, S., Rodriguez, J. J., & Bosco, G. (2012). Segmentation and detection of fluorescent 3D spots. *Cytometry A*, 81(3), 198-212. doi:10.1002/cyto.a.22017
- Ritchie, M. E., Phipson, B., Wu, D., Hu, Y., Law, C. W., Shi, W., & Smyth, G. K. (2015). limma powers differential expression analyses for RNA-sequencing and microarray studies. *Nucleic Acids Res*, 43(7), e47. doi:10.1093/nar/gkv007
- Romanov, R. A., Zeisel, A., Bakker, J., Girach, F., Hellysaz, A., Tomer, R., . . . Harkany, T. (2017). Molecular interrogation of hypothalamic organization reveals distinct dopamine neuronal subtypes. *Nat Neurosci*, 20(2), 176-188. doi:10.1038/nn.4462
- Sanz, E., Evanoff, R., Quintana, A., Evans, E., Miller, J. A., Ko, C., . . . McKnight, G. S. (2013). RiboTag analysis of actively translated mRNAs in Sertoli and Leydig cells in vivo. *PLoS One*, 8(6), e66179. doi:10.1371/journal.pone.0066179
- Sanz, E., Quintana, A., Deem, J. D., Steiner, R. A., Palmiter, R. D., & McKnight, G. S. (2015). Fertility-regulating Kiss1 neurons arise from hypothalamic POMC-expressing progenitors. *J Neurosci*, 35(14), 5549-5556. doi:10.1523/JNEUROSCI.3614-14.2015
- Sanz, E., Yang, L., Su, T., Morris, D. R., McKnight, G. S., & Amieux, P. S. (2009). Cell-type-specific isolation of ribosome-associated mRNA from complex tissues. *Proc Natl Acad Sci U S A*, 106(33), 13939-13944. doi:10.1073/pnas.0907143106
- Scott, N., Prigge, M., Yizhar, O., & Kimchi, T. (2015). A sexually dimorphic hypothalamic circuit controls maternal care and oxytocin secretion. *Nature*, 525(7570), 519-522. doi:10.1038/nature15378
- Smith, M. A., Makino, S., Kim, S. Y., & Kvetnansky, R. (1995). Stress increases brain-derived neurotrophic factor messenger ribonucleic acid in the hypothalamus and pituitary. *Endocrinology*, 136(9), 3743-3750. doi:10.1210/endo.136.9.7649080

- Stern, J. E., & Armstrong, W. E. (1998). Reorganization of the dendritic trees of oxytocin and vasopressin neurons of the rat supraoptic nucleus during lactation. *J Neurosci*, 18(3), 841-853.
- Su, B., Ji, Y. S., Sun, X. L., Liu, X. H., & Chen, Z. Y. (2014). Brain-derived neurotrophic factor (BDNF)-induced mitochondrial motility arrest and presynaptic docking contribute to BDNF-enhanced synaptic transmission. *J Biol Chem*, 289(3), 1213-1226.
doi:10.1074/jbc.M113.526129
- Suzuki, A., Matsumoto, Y., Shibuya, N., Sadahiro, R., Kamata, M., Goto, K., & Otani, K. (2011). The brain-derived neurotrophic factor Val66Met polymorphism modulates the effects of parental rearing on personality traits in healthy subjects. *Genes Brain Behav*, 10(4), 385-391. doi:10.1111/j.1601-183X.2010.00673.x
- Svare, B., & Mann, M. (1981). Infanticide: genetic, developmental and hormonal influences in mice. *Physiol Behav*, 27(5), 921-927.
- Tanaka, T., Saito, H., & Matsuki, N. (1997). Inhibition of GABAA synaptic responses by brain-derived neurotrophic factor (BDNF) in rat hippocampus. *J Neurosci*, 17(9), 2959-2966.
- Taniguchi, H., He, M., Wu, P., Kim, S., Paik, R., Sugino, K., . . . Huang, Z. J. (2011). A resource of Cre driver lines for genetic targeting of GABAergic neurons in cerebral cortex. *Neuron*, 71(6), 995-1013. doi:10.1016/j.neuron.2011.07.026
- Theodosios, D. T. (2002). Oxytocin-secreting neurons: A physiological model of morphological neuronal and glial plasticity in the adult hypothalamus. *Front Neuroendocrinol*, 23(1), 101-135. doi:10.1006/frne.2001.0226
- Timmusk, T., Belluardo, N., Persson, H., & Metsis, M. (1994). Developmental regulation of brain-derived neurotrophic factor messenger RNAs transcribed from different promoters in the rat brain. *Neuroscience*, 60(2), 287-291.

Timmusk, T., Palm, K., Metsis, M., Reintam, T., Paalme, V., Saarma, M., & Persson, H. (1993).

Multiple promoters direct tissue-specific expression of the rat BDNF gene. *Neuron*, 10(3), 475-489.

Unternaehrer, E., Meyer, A. H., Burkhardt, S. C., Dempster, E., Staehli, S., Theill, N., . . .

Meinlschmidt, G. (2015). Childhood maternal care is associated with DNA methylation of the genes for brain-derived neurotrophic factor (BDNF) and oxytocin receptor (OXTR) in peripheral blood cells in adult men and women. *Stress*, 18(4), 451-461.

doi:10.3109/10253890.2015.1038992

West, A. E., Pruunsild, P., & Timmusk, T. (2014). Neurotrophins: transcription and translation.

Handb Exp Pharmacol, 220, 67-100. doi:10.1007/978-3-642-45106-5_4

Wu, Z., Autry, A. E., Bergan, J. F., Watabe-Uchida, M., & Dulac, C. G. (2014). Galanin neurons in the medial preoptic area govern parental behaviour. *Nature*, 509(7500), 325-330.

doi:10.1038/nature13307

Wu, Z., Xu, Y., Zhu, Y., Sutton, A. K., Zhao, R., Lowell, B. B., . . . Tong, Q. (2012). An obligate role of oxytocin neurons in diet induced energy expenditure. *PLoS One*, 7(9), e45167.

doi:10.1371/journal.pone.0045167

Xu, X., Coats, J. K., Yang, C. F., Wang, A., Ahmed, O. M., Alvarado, M., . . . Shah, N. M.

(2012). Modular genetic control of sexually dimorphic behaviors. *Cell*, 148(3), 596-607.

doi:10.1016/j.cell.2011.12.018

Xu, Z., Lv, X. A., Dai, Q., Lu, M., & Jin, Z. (2017). Exogenous BDNF Increases Mitochondrial pCREB and Alleviates Neuronal Metabolic Defects Following Mechanical Injury in a

MPTP-Dependent Way. *Mol Neurobiol*. doi:10.1007/s12035-017-0576-5

Yamamoto, Y., Cushing, B. S., Kramer, K. M., Epperson, P. D., Hoffman, G. E., & Carter, C. S.

(2004). Neonatal manipulations of oxytocin alter expression of oxytocin and vasopressin immunoreactive cells in the paraventricular nucleus of the hypothalamus in a gender-

specific manner. *Neuroscience*, 125(4), 947-955.

doi:10.1016/j.neuroscience.2004.02.028

Yamashita, M., Glasgow, E., Zhang, B. J., Kusano, K., & Gainer, H. (2002). Identification of cell-specific messenger ribonucleic acids in oxytocinergic and vasopressinergic magnocellular neurons in rat supraoptic nucleus by single-cell differential hybridization. *Endocrinology*, 143(11), 4464-4476. doi:10.1210/en.2002-220516

Yu, G., Wang, L. G., Han, Y., & He, Q. Y. (2012). clusterProfiler: an R package for comparing biological themes among gene clusters. *OMICS*, 16(5), 284-287. doi:10.1089/omi.2011.0118

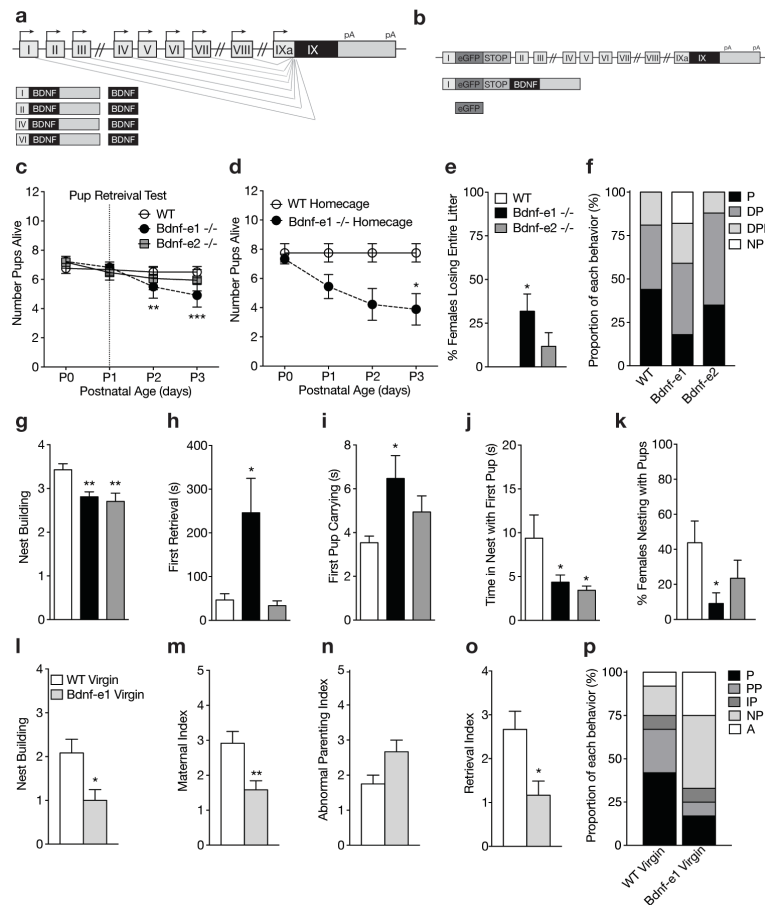


Figure 1. Disruption of BDNF from promoters I and II leads to impaired maternal care. **a**, Schematic of *Bdnf* transcript production. Transcription is initiated from promoters upstream of individual 5'-untranslated regions (UTRs) and spliced to the common coding exon IX. Each transcript produces an identical BDNF protein. **b**, Design of *Bdnf* $-/-$ mice using *Bdnf*-e1 $-/-$ as a representative example. Targeting vectors were designed to insert an enhanced green fluorescent protein (eGFP) upstream of the exon's splice donor site. *Bdnf*-e1 $-/-$ mice express a *Bdnf*-I-eGFP-STOP-*Bdnf* IX transcript leading to the production of GFP in lieu of BDNF. **c**, Average litter size over time for WT, *Bdnf*-e1 $-/-$, and *Bdnf*-e2 $-/-$ postpartum mothers exposed to the pup retrieval test one day after giving birth. *Bdnf*-e1 $-/-$ mothers show significant pup loss compared to WT mothers (2-way ANOVA with mixed effect model; $p < 0.001$). **d**, Average litter size over time for WT and *Bdnf*-e1 $-/-$ postpartum mothers remaining in the home cage. *Bdnf*-e1 $-/-$ mothers show significant pup loss compared to WT mothers even in a naturalistic setting (2-way ANOVA with mixed effect model; $p < 0.001$). **e**, Percentage of postpartum mothers losing their entire litter by postnatal day 3 (P3). Approximately 1/3 of postpartum *Bdnf*-e1 $-/-$ mothers lose their entire litter by P3 (1-way ANOVA with Bonferroni's multiple comparisons; $p < 0.05$). **f**, Proportion of WT, *Bdnf*-e1 $-/-$ and *Bdnf*-e2 $-/-$ with different maternal types including parenting (P), disorganized parenting (DP), partial parenting (PP), disorganized partial parenting (DPP), and non-parenting (NP). There is a significant decrease in the proportion of *Bdnf*-e1 $-/-$ postpartum mothers with parenting behavior compared to WT (one-tailed Mann-Whitney-Wilcoxon rank sum test, $p < 0.05$). *Bdnf*-e1 $-/-$ postpartum mothers show corresponding elevations in non-parenting behaviors. **g**, Bar graph depicting nest building behavior before parturition. *Bdnf*-e1 and -e2 $-/-$ show impaired nest building compared to WT (Kruskal-Wallis test with Dunn's multiple comparisons, $p < 0.01$). **h-j**, Latency to first retrieval (**h**), time carrying first pup (**i**), and time nesting with first pup (**j**) during the pup retrieval test. *Bdnf*-e1 $-/-$ postpartum mothers show increased latency to retrieval, longer time carrying the first pup to the nest, and reduced nesting time with first pup (1-way ANOVA with Bonferroni's multiple comparisons, $p < 0.05$). *Bdnf*-e2 $-/-$ postpartum mothers show similar, albeit milder phenotypes. **k**, Percentage of postpartum mothers successfully retrieving all pups and nesting for at least 2 continuous minutes. Significantly fewer *Bdnf*-e1 $-/-$ postpartum mothers successfully retrieve pups and continuously nest compared to WT (1-way ANOVA with Bonferroni's multiple comparisons, $p < 0.05$). **l**, Bar graph depicting nest building behavior of WT and *Bdnf*-e1 virgins 24 hours prior to pup retrieval test. *Bdnf*-e1 $-/-$ virgins show impairments in nest building compared to WT virgins (Mann-Whitney test, $p < 0.05$). **m-o**, Maternal (**m**), abnormal parenting (**n**), and retrieval (**o**) indices for WT and *Bdnf*-e1 $-/-$ virgins during foreign pup retrieval test. *Bdnf*-e1 $-/-$ virgin females show reductions in maternal and retrieval indices and a strong trend for increased abnormal parenting (Mann-Whitney tests, $p < 0.01$, $p < 0.05$, and $p = 0.0529$, respectively). **p**, Proportion of WT and *Bdnf*-e1 $-/-$ virgin females with different maternal types including parenting (P), partial parenting (PP), irregular parenting (IP), non-parenting (NP), and attack (A). There is a significant decrease in the proportion of *Bdnf*-e1 $-/-$ virgins with parenting behavior compared to WT. *Bdnf*-e1 $-/-$ virgins show corresponding elevations in attack behavior (one-tailed Mann-Whitney-Wilcoxon rank sum test, $p < 0.05$). Data are means \pm SEM. ($n = 16$ WT postpartum mothers; $n = 22$ *Bdnf*-e1 $-/-$ postpartum mothers; $n = 17$ *Bdnf*-e2 $-/-$ postpartum mothers; $n = 12$ WT virgins; $n = 12$ *Bdnf*-e1 $-/-$ virgins; * $p < 0.05$, ** $p < 0.01$, & $p < 0.001$, # $p < 0.0001$).

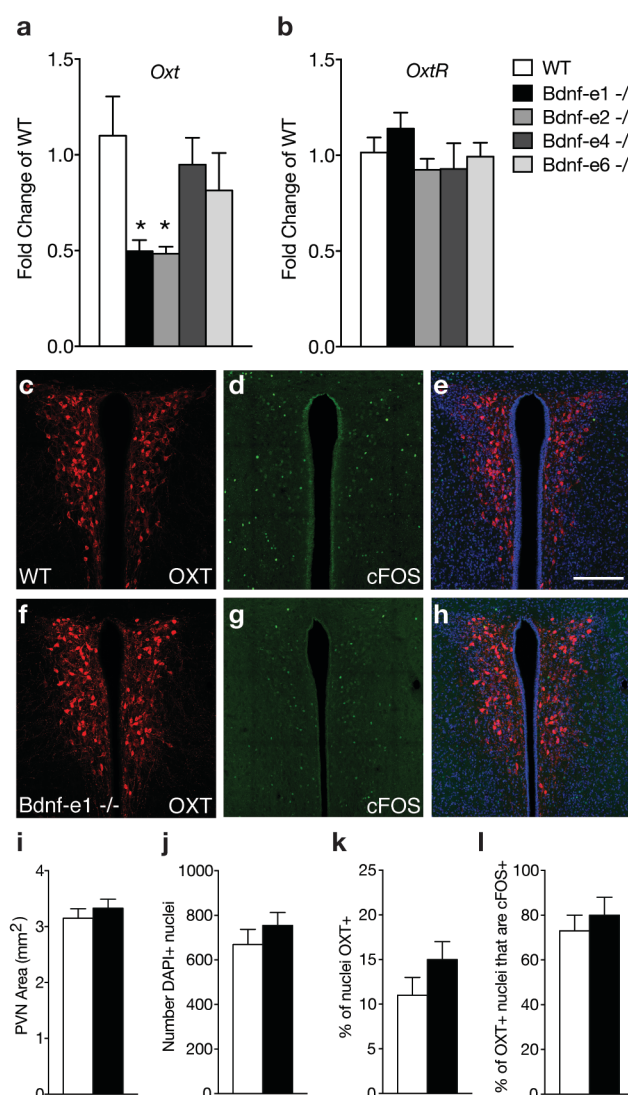


Figure 2. Oxytocin transcripts are reduced in Bdnf-e1 and -e2 -/- with impaired maternal care. **a-b**, qPCR demonstrating relative expression levels of oxytocin (**a**) and oxytocin receptor (**b**) transcripts in the HYP of 4 week old Bdnf-e1, -e2, -e4, and -e6 female mice (n=4-5 per genotype; 1-way ANOVAs with Bonferroni's multiple comparisons, $p < 0.05$). *Oxt*, but not *OxtR*, transcripts are reduced in Bdnf-e1 and -e2 -/- females. **c-h**, Confocal z-projections of PVN from WT (**c-e**) and Bdnf-e1 -/- (**f-h**) postpartum mothers collected 2 hours following pup retrieval testing. Immunolabeling of OXT (**c, f**) cFOS (**d, g**), and merged images (**e, h**). **i-l**, Quantification of PVN area (**i**), number of PVN cells (**j**), % of PVN cells expressing OXT (**k**), and percentage of OXT neurons expressing cFOS following pup retrieval (**l**) in WT and Bdnf-e1 -/- postpartum mothers (n= 6-9 images per animal; n=3 animals per genotype; student's *t*-test, Poisson regression, and binomial regression, respectively). There were no significant differences in PVN structure, OXT neuron number, or proportion of OXT neurons activated following pup retrieval. Data are means \pm SEM; * $p < 0.05$.

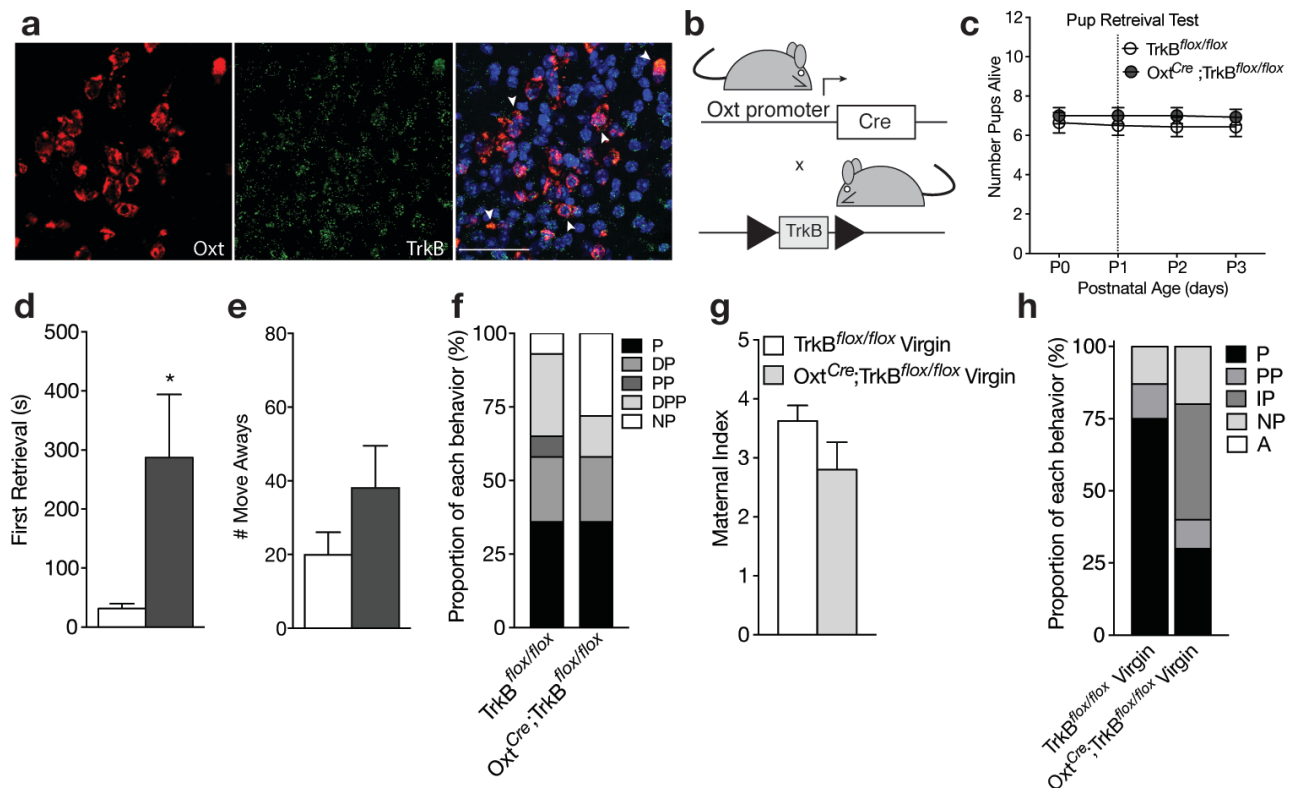


Figure 3. Loss of TrkB in OXT neurons leads to parenting deficits in postpartum mothers and virgin females. **a**, Confocal z-projections of *Oxt* and *Ntrk2* transcripts in brain slices containing the PVN from an adult female visualized with RNAscope *in situ* hybridization. TrkB transcripts (green) are highly expressed in OXT neurons (red). **b**, Breeding strategy used to obtain *Oxt^{Cre}; TrkB^{flox/flox}* mice. **c**, Average litter size over time for *TrkB^{flox/flox}* and *Oxt^{Cre}; TrkB^{flox/flox}* postpartum mothers exposed to the pup retrieval test one day post parturition. Mothers lacking TrkB in OXT neurons show normal pup survival compared to control (2-way ANOVA with mixed effect model; $p > 0.05$). **d**, Latency to first retrieval during pup retrieval test. *Oxt^{Cre}; TrkB^{flox/flox}* postpartum mothers show increased latency to retrieve first pup (Student's *t*-test; $p < 0.05$). **e**, Number of times postpartum mothers move away from pups without retrieving. *Oxt^{Cre}; TrkB^{flox/flox}* mothers show a strong trend for increased move-aways. **f**, Proportion of *Oxt^{Cre}; TrkB^{flox/flox}* and control mothers with different maternal types including parenting (P), disorganized parenting (DP), partial parenting (PP), disorganized partial parenting (DPP), and non-parenting (NP). There is no significant change in the proportion of *Oxt^{Cre}; TrkB^{flox/flox}* mothers with parenting behavior compared to control (one-tailed Mann-Whitney-Wilcoxon rank sum test, $p > 0.05$). However, a substantial proportion of *Oxt^{Cre}; TrkB^{flox/flox}* mothers show non-parenting behaviors. **g**, Maternal index for control and *Oxt^{Cre}; TrkB^{flox/flox}* virgin females during foreign pup retrieval test. *Oxt^{Cre}; TrkB^{flox/flox}* virgin females show a trend for reduced maternal index. **h**, Proportion of *Oxt^{Cre}; TrkB^{flox/flox}* and control mothers with different maternal types including parenting (P), partial parenting (PP), irregular parenting (IP), non-parenting (NP), and attack (A). There is a significant decrease in the proportion of *Oxt^{Cre}; TrkB^{flox/flox}* virgins with parenting behavior compared to control (one-tailed Mann-Whitney-Wilcoxon rank sum test, $p < 0.05$). Data are means \pm SEM. ($n = 14$ *TrkB^{flox/flox}* postpartum mothers; $n = 14$ *Oxt^{Cre}; TrkB^{flox/flox}* postpartum mothers; $n = 8$ *TrkB^{flox/flox}* virgins; $n = 10$ *Oxt^{Cre}; TrkB^{flox/flox}* virgins; $*p < 0.05$).

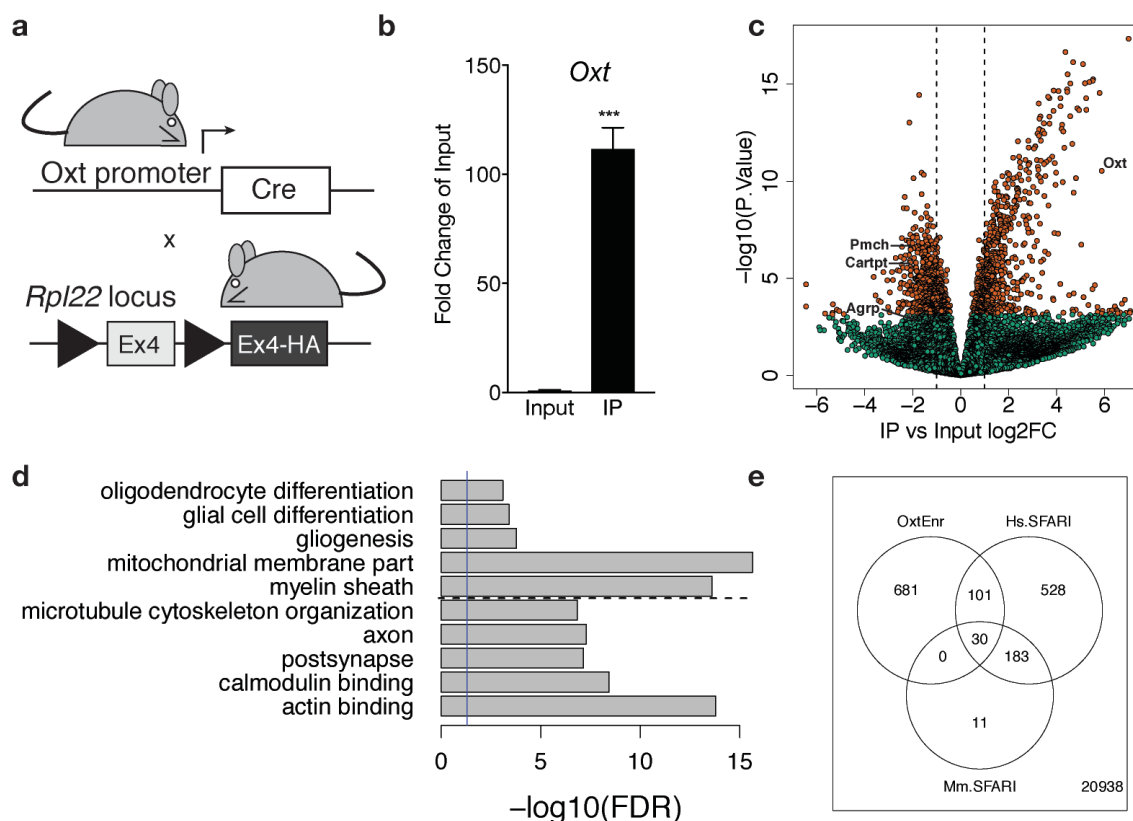


Figure 4. Identification of a unique molecular profile for OXT neurons using ribosomal tagging. **a**, Locus of the ribosomal protein *Rpl22* in the Ribotag mouse and breeding strategy used to obtain *Oxt^{Cre}; Rpl22^{HA}* mice. **b**, qPCR analysis validating significant enrichment of *Oxt* transcripts in IP compared to Input fractions. **c**, Volcano plot of RNA-seq results with IP versus Input log₂ fold change against $-\log_{10}$ p-value. Outer lines are 2-fold enriched/depleted genes. Red dots represent genes that are significantly different (<0.05) in IP versus Input. Green dots represent non-significant genes. A subset of differentially enriched marker genes is highlighted (*Oxt*, *AgRP*, *Cartpt*, *Pmch*). **d**, Representative gene ontology (GO) terms in the cellular component, molecular function and biological processes categories for genes enriched and depleted in OXT neurons. Solid vertical line indicates $p=0.05$ and dotted horizontal line separates downregulated (top) and upregulated (bottom) pathways. **e**, Venn diagram showing overlap of differentially expressed genes (DEGs) in OXT neurons with mouse (Mm) and human (Hs) genes implicated in autism spectrum disorder by the Simons Foundation Autism Research Initiative (SFARI). Data are means \pm SEM. ($n=3$ Input, $n=3$ IP; 5 *Oxt^{Cre}; Rpl22^{HA}* hypothalami pooled per sample).

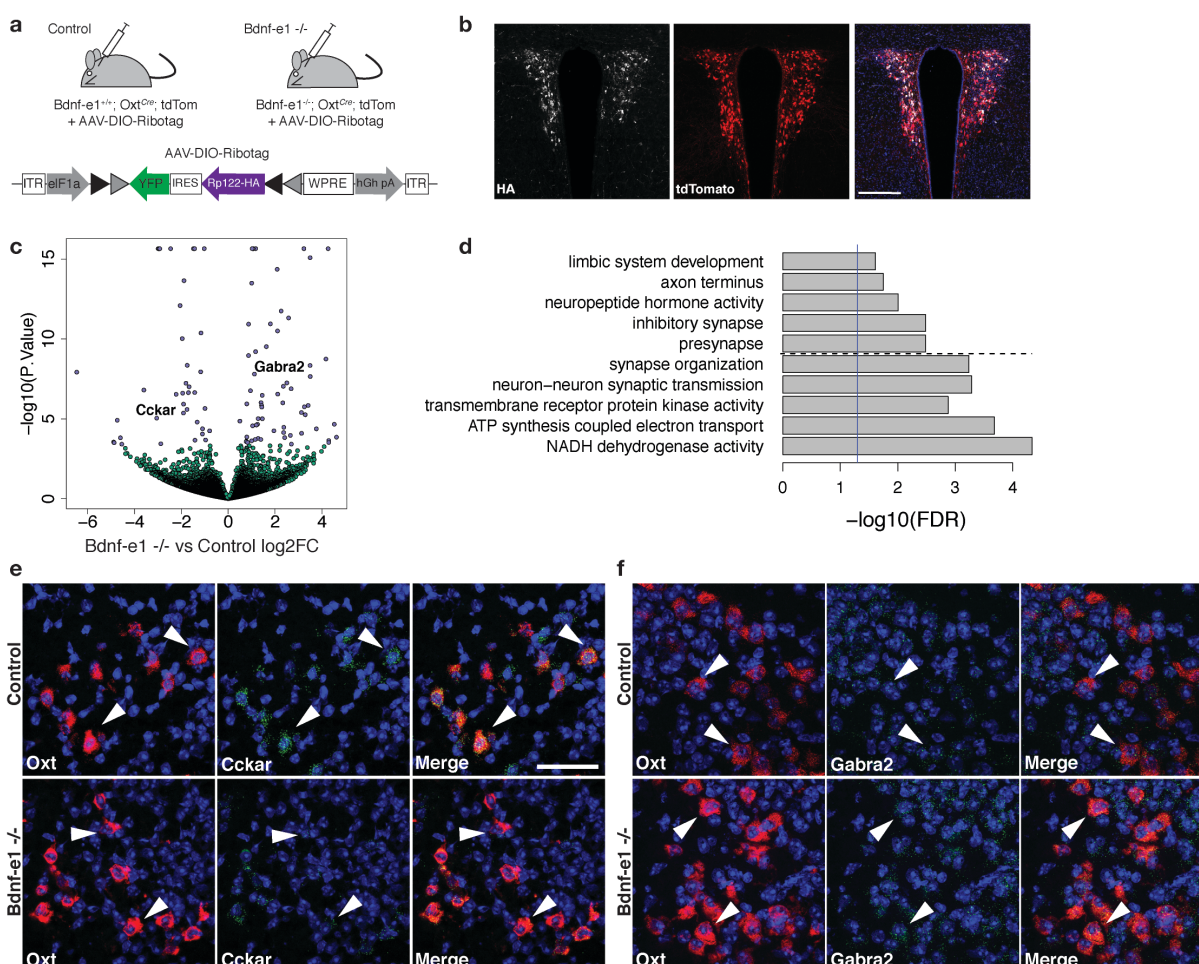


Figure 5. Perturbations in BDNF signaling impact gene pathways critical for plasticity in OXT neurons. **a**, Strategy for TRAP in OXT neurons from control and Bdnf-e1^{-/-} mice (n=3 per genotype) using AAV-DIO-RiboTag and RNA-seq. **b**, Confocal image showing HA (white) and tdTomato (red) expression in hypothalamic sections containing the PVN of Bdnf-e1^{-/-}; Oxt^{Cre}; tdTom mice injected bilaterally with AAV-DIO-RiboTag. Scale bar is 200μm. **c**, Volcano plot of RNA-seq results with Bdnf-e1^{-/-} IP vs. control IP log₂ fold change against -log₁₀ p-value. Blue dots represent genes that are significantly different in Bdnf-e1^{-/-} IP vs. control IP, including *Cckar* and *Gabra2*. Green dots represent non-significant genes. **d**, Representative gene ontology (GO) terms in the molecular function, biological processes, and cellular component categories for genes enriched and de-enriched in OXT neurons following disruption of BDNF signaling. Solid vertical line indicates p=0.05 and dotted horizontal line separates downregulated (top) and upregulated (bottom) pathways. **e**, Confocal z-projections of *Oxt* and *Cckar* transcripts in brain slices containing the PVN from adult control and Bdnf-e1^{-/-} females visualized with RNAscope *in situ* hybridization. *Cckar* transcripts (green) are enriched in *Oxt*-expressing neurons (red) in control, but not Bdnf-e1^{-/-} females. **f**, Confocal z-projections of *Oxt* and *Gabra2* transcripts in adult PVN of control and Bdnf-e1^{-/-} females visualized with RNAscope *in situ* hybridization. *Gabra2* transcripts (green) co-localize with *Oxt* transcripts (red) in control females and appear elevated in Bdnf-e1^{-/-} females. Scale bar is 50μm.

SUPPLEMENTARY INFORMATION

Supplementary Methods

Estrous testing

Virgin WT and Bdnf-e1 ^{-/-} female mice aged 7-8 weeks received vaginal cytology smears for 10 consecutive days at 2pm to determine estrous cycle patterns. Briefly, 100µl of sterile saline was used to collect vaginal cells in a graduated pipette tip. Samples were placed in a cell culture well and assayed under a light microscope. Cell density and cytoarchitecture were used to classify estrous stage: proestrous (P), estrous (E), or diestrous/metestrous (D/M) as previously described (McLean et al 2012).

Sexual receptivity/mating experiments

WT and Bdnf-e1 ^{-/-} virgin females accustomed to handling associated with vaginal cytology smears were subjected to mating experiments. Females determined to be in estrous by characterization of vaginal cells were placed in a cage with a CD1 male mouse at the start of the dark cycle (6pm). Using infrared lights and CaptureStar software (CleverSystems), male-female interactions were video-recorded for 30 minutes. Duration of time spent exploring the cage or being chased/cornered by males was hand-scored with experimenter blinded to genotype. Number of female rejections (i.e. kicking, biting, lordosis failure) was also scored.

Supplementary Figures and Legends (Figures S1-S4)

Supplementary Tables and Legends (Tables S1-S8)

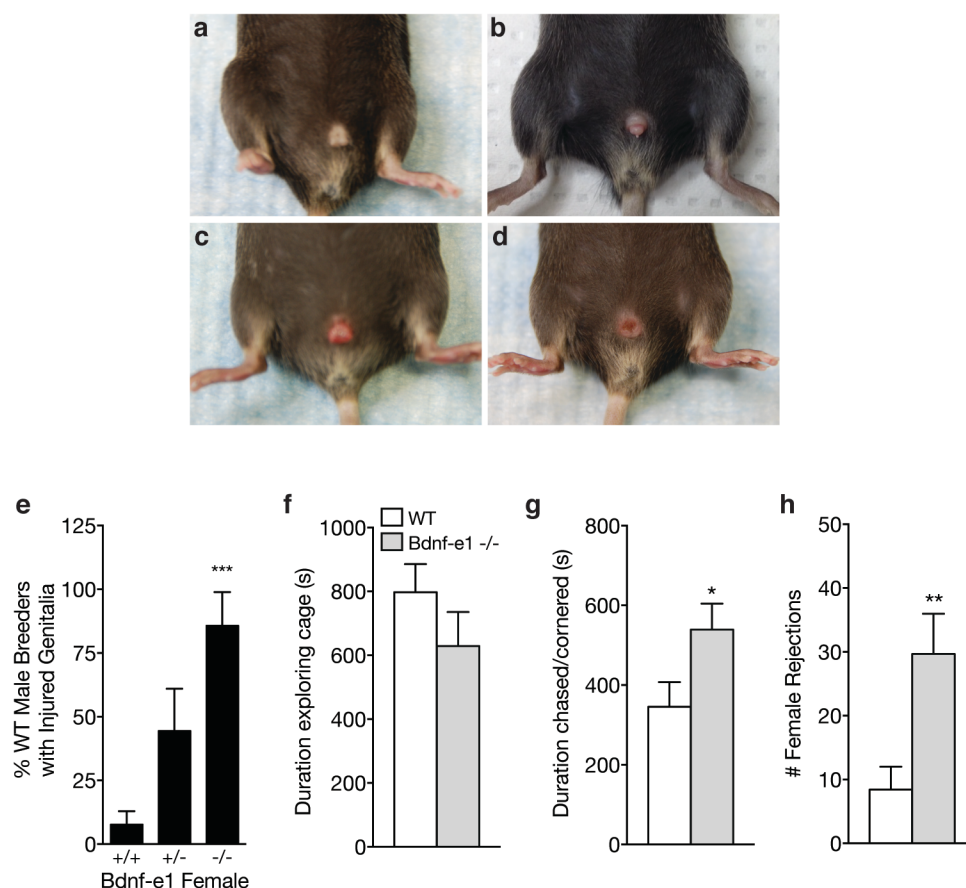


Figure S1. Bdnf-e1 -/- females show abnormal mating behaviors. **a-d**, Representative images depicting male genitalia injuries observed in Bdnf-e1 breeder cages. Breeder males frequently show inflamed, infected, and/or mutilated genitalia (**b-d**) compared to normal (**a**) when paired with heterozygous or homozygous Bdnf-e1 females. **e**, Bar graph depicting the percentage of WT male breeders with injured genitalia when paired with females that are wild-type, heterozygous, or homozygous for promoter I-derived BDNF production. WT males rarely show injuries when paired with WT females; however, partial or complete loss of promoter I-derived BDNF leads to significant increases in injured males (1-way ANOVA; $n = 26$ +/+, $n = 9$ +/-, $n = 7$ -/-; $p < 0.001$). **f-h**, Quantification of mating behaviors between WT ($n = 12$) or Bdnf-e1 -/- ($n = 12$) estrous females and CD1 males, including duration exploring (**f**), duration chased/cornered (**g**), and number of female rejections (**h**). WT and Bdnf-e1 -/- females spend equal time exploring; however, Bdnf-e1 -/- females are more frequently cornered or chased by males (Student's t test, $p < 0.05$). Bdnf-e1 -/- females also show a significant increase in mounting rejections (Student's t test, $p < 0.01$). Data are means \pm SEM; * $p < 0.05$, ** $p < 0.01$.

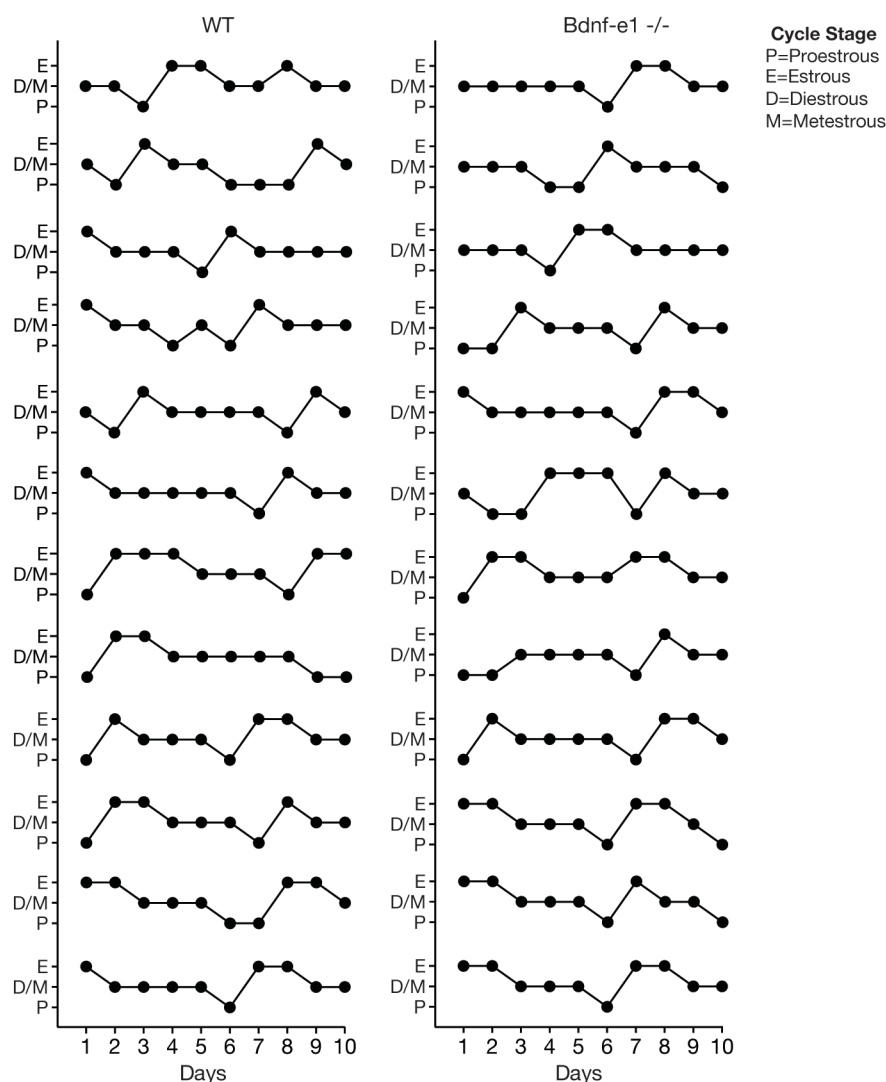


Figure S2. Bdnf-e1 -/- females have a normal estrous cycle. Bdnf-e1 -/- virgin females enter all stages of the estrous cycle, including proestrous (P), estrous (E), diestrus (D), and metestrous (M), similar to WT females. Bdnf-e1 -/- virgins enter estrous ~every 5 days and remain in estrous for 24- 48 hours.

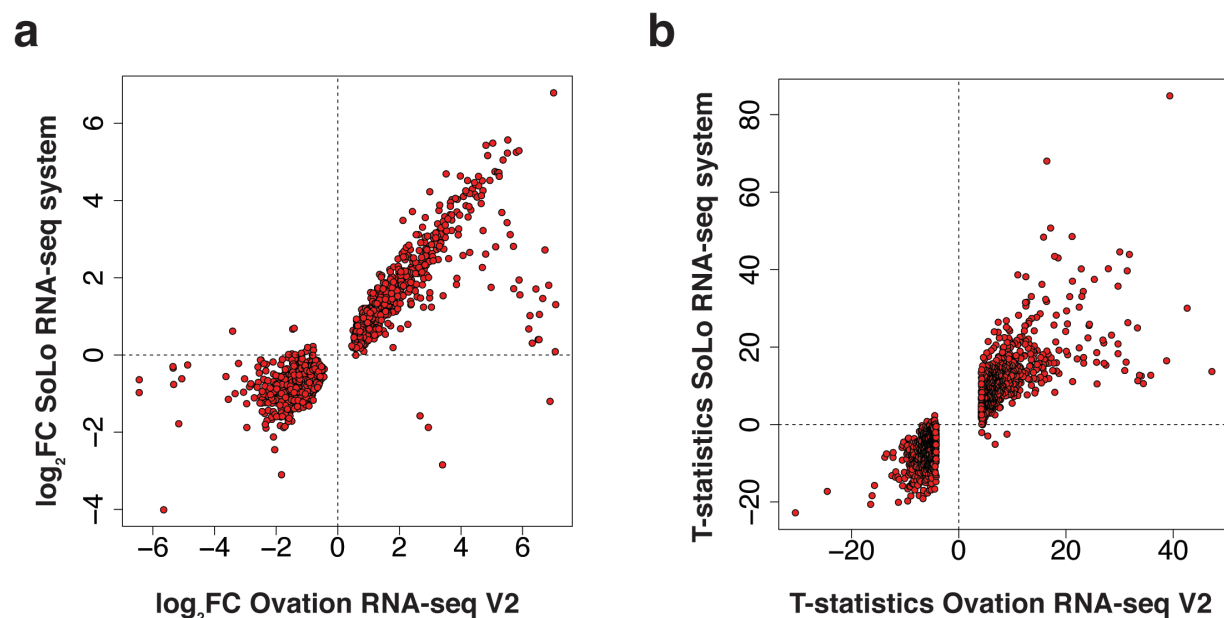


Figure S3. Validation of Ovation RNA-seq V2 system with SoLo RNA-seq system.

a, Plot depicting \log_2 fold changes of DEGs in Oxt IP vs. Oxt Input using RNA-seq V2 system compared to the SoLo RNA-seq system. Fold changes are highly correlated between kits. **b**, Plot depicting t-statistics for Oxt IP vs. Oxt Input using RNA-seq V2 system compared to SoLo RNA-seq system shows strong consistency between kits.

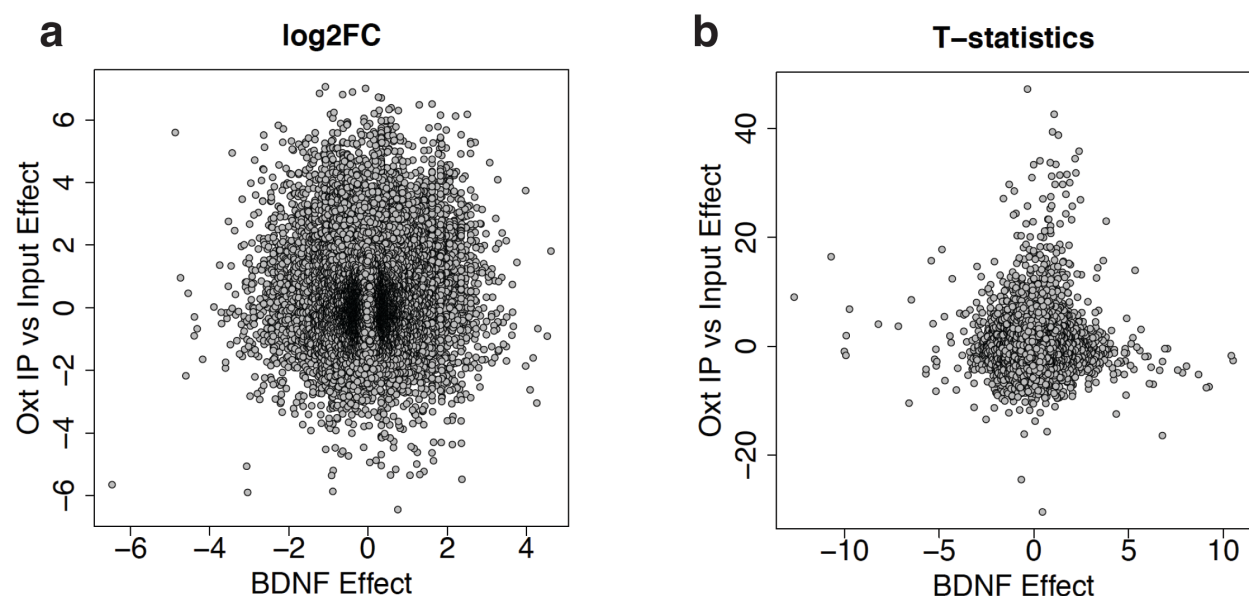


Figure S4. DEGs in Oxt Input vs. Oxt IP do not overlap with DEGs in control IP vs. Bdnf-e1 -/-IP. **a**, Plot depicting \log_2 fold changes of DEGs in Oxt IP vs. Oxt Input compared to the \log_2 fold changes of DEGs in control IP vs. Bdnf-e1 -/- IP. As expected, there is no correlation between the two sets of DEGs. **b**, Plot depicting t-statistics for Oxt IP vs. Oxt Input compared to t-statistics for control IP vs. Bdnf-e1 -/- IP.

Supplemental Table Legends (Excel tables attached as separate tabs in a single file)

Table S1. Differential gene expression analysis of OXT Input vs. IP samples.

Table S2. Comparison of OXT neuron gene enrichment using Nugen Ovation RNA-seq System V2 kit vs. Nugen Ovation SoLo RNA-seq system. Table also includes comparison of differential gene expression between Oxt neurons, Cst inhibitory interneurons, and Ntsr1 layer VI corticothalamic neurons.

Table S3. Gene Ontology analysis in OXT neurons. Enriched and depleted GO terms from differential expression analysis of OXT Input vs. IP.

Table S4. OXT enriched mouse model genes in SFARI. List of genes enriched in OXT neurons implicated in genetic animal models of autism spectrum disorder (ASD) by the Simons Foundation Autism Research Initiative (SFARI).

Table S5. OXT enriched human genes in SFARI. List of genes enriched in OXT neurons implicated in ASD by the SFARI Human Gene Module using the subset of mouse-expressed genes with human homologs.

Table S6. Differential gene expression analysis of control IP vs. Bdnf-e1 -/- IP.

Table S7. Gene Ontology analysis in OXT neurons with disruption of BDNF signaling. GO terms enriched from differential expression analysis of control IP vs. Bdnf-e1 -/- IP samples.

Table S8. BDNF-dependent OXT genes in SFARI. List of genes perturbed in OXT neurons following disruption of BDNF signaling that are implicated in autism spectrum disorder (ASD) by the Simons Foundation Autism Research Initiative (SFARI).